

# ACRONYM III: Radial Velocities for 336 Candidate Young Low-Mass Stars in the Solar Neighborhood, Including 77 Newly Confirmed Young Moving Group Members

ADAM C. SCHNEIDER,<sup>1</sup> EVGENYA L. SHKOLNIK,<sup>1</sup> KATELYN N. ALLERS,<sup>2</sup> ADAM L. KRAUS,<sup>3</sup> MICHAEL C. LIU,<sup>4</sup>  
ALYCIA J. WEINBERGER,<sup>5</sup> AND LAURA FLAGG<sup>6</sup>

<sup>1</sup>*School of Earth and Space Exploration, Arizona State University, Tempe, AZ, 85282, USA*

<sup>2</sup>*Department of Physics and Astronomy, Bucknell University, Lewisburg, PA 17837, USA*

<sup>3</sup>*The University of Texas at Austin, Department of Astronomy, Austin, TX 78712, USA*

<sup>4</sup>*Institute for Astronomy, University of Hawaii, Honolulu, HI 96822, USA*

<sup>5</sup>*Department of Terrestrial Magnetism, Carnegie Institution of Washington, Washington, DC 20015, USA*

<sup>6</sup>*Physics & Astronomy Department, Rice University, Houston, TX 77005, USA*

(Received; Accepted)

Submitted to AJ

## ABSTRACT

Young, low-mass stars in the solar neighborhood are vital for completing the mass function for nearby, young coeval groups, establishing a more complete census for evolutionary studies, and providing targets for direct-imaging exoplanet and/or disk studies. We present properties derived from high-resolution optical spectra for 336 candidate young nearby, low-mass stars. These include measurements of radial velocities and age diagnostics such as H $\alpha$  and Li  $\lambda$ 6707 equivalent widths. Combining our radial velocities with astrometry from *Gaia* DR2, we provide full 3D kinematics for the entire sample. We combine the measured spectroscopic youth information with additional age diagnostics (e.g., X-ray and UV fluxes, CMD positions) and kinematics to evaluate potential membership in nearby, young moving groups and associations. We identify 77 objects in our sample as bonafide members of 10 different moving groups, 14 of which are completely new members or have had their group membership reassigned. We also reject 46 previously proposed candidate moving group members. Furthermore, we have newly identified or confirmed the youth of numerous additional stars that do not belong to any currently known group, and find 69 co-moving systems using *Gaia* DR2 astrometry. We also find evidence that the Carina association is younger than previously thought, with an age similar to the  $\beta$  Pictoris moving group ( $\sim$ 22 Myr).

*Keywords:* stars: low-mass

## 1. INTRODUCTION

The discovery of young stars ( $<300$  Myr) in the neighborhood of the Sun ( $<100$  pc) has allowed for significant advances in several areas of astrophysics. Because of their age and proximity, such stars are optimal targets for directly detecting low-mass planetary companions (e.g., Chauvin et al. 2004, 2005, Marois et al. 2008, 2010, Lagrange et al. 2010, Bowler et al. 2013, 2017, Naud et al. 2014, Chauvin et al. 2017, Dupuy et al.

2018), in-depth studies of circumstellar disks (e.g., Su et al. 2006, Rebull et al. 2008, Zuckerman et al. 2011, Riviere-Marichalar et al. 2014, Rodriguez et al. 2015, Binks & Jeffries 2017, Meng et al. 2017), mass function investigations (e.g., Kraus et al. 2014, Shkolnik et al. 2017, Gagné et al. 2017a), and studies of various evolutionary properties ranging from rotation and activity (e.g., Montes et al. 2001 de la Reza & Pinzón 2004, Malo et al. 2014, Shkolnik & Barman 2014, Schneider & Shkolnik 2018) to chemical abundances (e.g., Mentuch et al. 2008, da Silva et al. 2009, Viana Almeida et al. 2009, Žerjal et al. 2019) to multiplicity (e.g., Janson et al. 2014, Shan et al. 2017) to empirical isochrones (e.g., Liu et al. 2016).

Nearby, young moving groups are coeval collections of stars that share the same age and similar space motions (e.g., [Kastner et al. 1997](#)). Confirming membership to these kinematically linked groups requires knowledge of an object’s distance, proper motion, radial velocity, and age. While proper motions have typically been available from numerous all-sky surveys, accurate distances and radial velocities have been more difficult to acquire as they require dedicated observations. With the second data release of the *Gaia* mission (hereafter *Gaia* DR2; [Gaia Collaboration et al. 2016, 2018](#)), parallaxes are now readily available for the vast majority of nearby, stellar moving group members. Such data is being used to identify new moving group members as well as completely new moving groups (e.g., [Faherty et al. 2018](#), [Gagné et al. 2018d](#)). In many instances, the only pieces of information now missing to confirm a potential moving group member are its radial velocity and youth. The *Gaia* mission will eventually include radial velocities for  $\sim 150$  million stars ([Soubiran et al. 2018](#)), and the DR2 release includes radial velocities for over 7 million bright stars, though with increasing uncertainties at the faint end ( $\gtrsim 2$  km s $^{-1}$ ; [Gaia Collaboration et al. 2018](#)). In this third installment of the All-sky Co-moving Recovery Of Nearby Young Members (ACRONYM) series ([Kraus et al. 2014](#), [Shkolnik et al. 2017](#)), we present radial velocities and youth characteristics for 336 nearby, low-mass stars that are suspected to be young in order to identify new, and confirm previously proposed, moving group members.

## 2. OBSERVATIONS

Nearby young candidates were observed with the goal of identifying young, nearby, low-mass stars. These include the list of X-ray active M dwarfs from the NStars catalog ([Reid et al. 2003, 2004](#)) and from [Riaz et al. \(2006\)](#), kinematic moving group candidates from [Malo et al. \(2013\)](#), and UV-active M dwarfs using the methods outlined in [Shkolnik et al. \(2011\)](#). For X-ray active M dwarfs, we required the log of the X-ray flux ( $F_X$ ) to 2MASS *J*-band flux ( $F_J$ ) to be greater than  $-2.5$ , a value chosen to be comparable to members of the Pleiades ([Shkolnik et al. 2009](#)). For UV-active M dwarf candidates, we required  $3\sigma$  detections in both the *GALEX* FUV and NUV bands, and required the FUV and NUV to 2MASS *J*-band flux ratios to be greater than  $10^{-5}$  and  $10^{-4}$ , respectively ([Shkolnik et al. 2011](#)). High resolution optical spectra were acquired for all targets to measure radial velocities and youth diagnostics. Radial velocity standards were observed each night in order to determine radial velocities of our target stars. Care was

taken to observe radial velocity standards with similar spectral types as the target sample. All observations are summarized in Table 1.

### 2.1. Keck/HIRES

Fifty-two targets were observed with the High Resolution Echelle Spectrometer (HIRES; [Vogt et al. 1994](#)) on the Keck I telescope. The observing strategy and data reduction routine are outlined in [Shkolnik et al. \(2009, 2017\)](#), which we briefly summarize here. All observations were taken with the  $0''.861$  slit, resulting in a spectral resolution of  $\lambda/\Delta\lambda \approx 58,000$  covering a wavelength range of 4900–9300 Å. The GG475 filter was utilized with the red cross-disperser in order to maximize the throughput at the longest wavelengths (where M dwarfs emit their peak emission). All data reduction was accomplished using the facility pipeline MAKEE.

### 2.2. CFHT/ESPaDONs

We observed 15 targets with the Echelle SpectroPolarimetric Device for the Observation of Stars (ESPaDONs; [Donati et al. 2006](#)) on the Canada-France-Hawaii Telescope (CFHT). The observing strategy and data reduction routine are outlined in [Shkolnik et al. \(2009\)](#), which we briefly summarize here. ESPaDONs covers a wavelength range of 3700–10400 Å, with a spectral resolution of  $\lambda/\Delta\lambda \approx 68,000$ . Data reduction was achieved using the fully automated reduction package *Libre ESPrIT* ([Donati et al. 2007](#)).

### 2.3. Magellan/MIKE

The Magellan Inamori Kyocera Echelle (MIKE) optical spectrograph located on the Clay telescope at the Magellan Observatory was used to characterize 122 of our targets. The observing strategy and data reduction routine are outlined in [Shkolnik et al. \(2011, 2017\)](#), which we briefly summarize here. We used the  $0''.5$  slit with for all MIKE observations, which gives a spectral resolution of  $\lambda/\Delta\lambda \approx 35,000$  over the wavelength range 4900–10000 Å. All MIKE data were reduced using the CarPy pipeline ([Kelson et al. 2000; Kelson 2003](#)).

### 2.4. Du Pont/Echelle

Two-hundred and twenty-nine targets were observed with the Echelle Spectrograph on the 2.5 m Irene Du Pont Telescope. All observations were taken with a  $1''.0$  slit, resulting in a resolution of  $\lambda/\Delta\lambda \approx 32,000$  covering the 4000–9000 Å wavelength range. Standard IRAF echelle routines were used to reduce the data.

**Table 1.** Observations Summary

2MASS Designation	Other Name	Telescope/ Instrument	Obs. Date (UT)	RV (km s <sup>-1</sup> )	SB?
00153670–2946003	GJ 3017	Magellan/MIKE	2009 Dec 31	0.61±1.31	...
00213729–4605331	GJ 3029	Magellan/MIKE	2009 Jun 06	-19.32±0.12	...
00254902+4501315	[FS2003] 0016	Keck/HIRES	2012 Dec 28	6.30±0.32	...
00354412–0541102	LP 645-53	Magellan/MIKE	2009 Jun 07	-15.63±0.17	...
00501079–0337532	...	Magellan/MIKE	2010 Jan 01	0.27±1.24	...
00503319+2449009	GJ 3061	DuPont/Echelle	2009 Aug 21	5.42±0.38	...
00503319+2449009	GJ 3061	Magellan/MIKE	2009 Dec 31	7.44±1.24	...
00503319+2449009	GJ 3061	Magellan/MIKE	2009 Dec 31	7.53±1.58	...
00503319+2449009	GJ 3060	Magellan/MIKE	2009 Dec 31	5.60±0.79	...
00503319+2449009	GJ 3060	Magellan/MIKE	2009 Dec 31	5.64±0.87	...
00560596+4153282	...	Keck/HIRES	2013 Oct 24	-33.12±0.17	...
01031408+2005523	GJ 1026 A	DuPont/Echelle	2009 Aug 21	21.51±0.38	...
01031408+2005523	GJ 1026 B	DuPont/Echelle	2009 Aug 21	21.87±0.41	SB±
01031408+2005523	GJ 1026 B	Magellan/MIKE	2009 Dec 31	20.11±0.92	SB±
01031408+2005523	GJ 1026 B	Magellan/MIKE	2009 Dec 31	21.53±0.39	SB±
01050677+2815049	1RXS J010506.0+281505	Keck/HIRES	2013 Oct 24	3.85±0.39	...
01090150–5100494	DG Phe	Magellan/MIKE	2009 Jun 08	-1.15±0.81	...
01112542+1526214	GJ 3076	Keck/HIRES	2012 Dec 28	2.84±0.12	...
01132401–2254077	GJ 1033	DuPont/Echelle	2013 Dec 19	-0.13±0.80	...
01132958–0738088	StKM 1-124	DuPont/Echelle	2013 Dec 18	115.97±2.37	SB1
01205998–2408520	BPS CS 29514-0033	Magellan/MIKE	2009 Jun 07	3.48±5.98	...
01210504–0402082	G 271-42	Magellan/MIKE	2010 Jan 01	9.30±1.83	...
01244246–1540454	G 272-13	DuPont/Echelle	2013 Dec 18	18.09±0.60	...
01245068–3844389	SERC 296A	Magellan/MIKE	2011 Jun 14	16.20±0.51	...
01302034–2557105	GSC 06426-01758	Magellan/MIKE	2009 Jun 07	13.56±0.24	...
01335800–1738235	LP 768-113	Magellan/MIKE	2010 Jan 01	5.87±0.28	...
01345037–0254397	...	Magellan/MIKE	2010 Jan 01	-11.27±1.46	...
01452133–3957204	CD-40 436	DuPont/Echelle	2013 Dec 18	21.06±0.59	...
01484087–4830519	GSC 08044-00859	Magellan/MIKE	2010 Jan 01	21.32±0.31	...
01511997+1324525	[ZEH2003] RX J0151.3+1324 3	Magellan/MIKE	2010 Jan 01	25.96±0.42	...
01564714–0021127	GSC 04686-00596	Magellan/MIKE	2010 Jan 01	3.43±1.33	...
02130073+1803460	LP 409-52	DuPont/Echelle	2009 Aug 21	2.68±0.43	SB±
02130073+1803460	LP 409-52	Magellan/MIKE	2009 Dec 31	2.97±0.61	SB±
02133021–4654505	WISE J021330.24-465450.3	Magellan/MIKE	2010 Jan 01	10.33±1.02	...
02135155–4129304	CD-42 759	DuPont/Echelle	2013 Dec 18	8.33±1.09	...
02135155–4129304	CD-42 759	DuPont/Echelle	2013 Dec 18	10.28±1.93	...
02165488–2322133	1RXS J021655.0-232216	Magellan/MIKE	2010 Jan 01	3.81±2.53	...
02202235–0808253	LP 650-215	Keck/HIRES	2013 Oct 24	3.37±1.07	...
02291365–1009419	...	Magellan/MIKE	2010 Jan 01	12.94±0.40	...

*Table 1 continued*

Table 1 (continued)

2MASS Designation	Other Name	Telescope/ Instrument	Obs. Date (UT)	RV (km s <sup>-1</sup> )	SB?
02344773–2222451	...	Magellan/MIKE	2010 Jan 01	8.36±1.70	...
02371574–2222590	...	Magellan/MIKE	2010 Jan 01	3.54±0.44	...
02374615–0705480	LHS 1427	Keck/HIRES	2013 Oct 24	-8.01±0.08	...
02390078–1937040	...	Magellan/MIKE	2010 Jan 01	23.41±0.69	...
02411909–5725185	GSC 08494-00369	Magellan/MIKE	2010 Jan 01	7.03±0.43	...
02411909–5725185	GSC 08494-00369	Magellan/MIKE	2010 Jan 01	8.68±0.60	...
02442137+1057411	MCC 401	DuPont/Echelle	2013 Dec 20	5.60±1.09	...
02445715–4407313	...	Magellan/MIKE	2010 Jan 01	16.79±0.67	...
02461477–0459182	GJ 3180	Magellan/MIKE	2009 Jun 07	35.00±0.22	...
02490228–1029220	UCAC4 398-003401	Magellan/MIKE	2010 Jan 01	16.85±0.43	...
02492136–4416063	...	Magellan/MIKE	2010 Jan 01	29.06±0.31	...
02511150–4753077	GSC 08054-00859	DuPont/Echelle	2013 Dec 19	-15.11±0.88	...
02523096–1548357	...	Keck/HIRES	2012 Dec 28	73.68±0.59	...
02535980+3206373	...	Keck/HIRES	2006 Aug 12	-36.26±0.81	SB1
02535980+3206373	...	Keck/HIRES	2012 Dec 28	-34.64±0.17	SB1
02545247–0709255	...	Keck/HIRES	2012 Dec 28	25.11±0.18	SB2
02560388–0036332	LP 591-156	DuPont/Echelle	2009 Aug 21	46.29±0.38	SB1
02560388–0036332	LP 591-156	Magellan/MIKE	2009 Dec 31	46.04±0.40	SB1
03033668–2535329	CD-26 1122	Magellan/MIKE	2012 Jan 16	16.94±0.71	...
03051118–3405239	LP 942-107	DuPont/Echelle	2013 Dec 18	24.32±0.64	...

NOTE—Table 1 is available in its entirety in a machine-readable form in the online journal. A portion is shown here for guidance regarding its form and content.

### 3. ANALYSIS

#### 3.1. Spectral Types

Spectral types are taken from the literature, with references given in Table 2. For those objects without an available spectral type, we measure the type using the TiO5 index defined in Reid et al. (1995). The spectral type distribution of the entire sample is shown in Figure 1.

#### 3.2. Radial Velocities

One of the main objectives of this work is to measure radial velocities for potentially young, nearby, low mass stars. For each of our high-resolution spectra, we isolate the reddest orders ( $\gtrsim 7000$  Å) for radial velocity measurements as that is where the signal to noise ratio (S/N) is highest for low mass stars. Each order was cross-correlated with radial velocity standards of similar spectral type using the *fxcor* routine from IRAF. Radial velocities were measured by finding the Gaussian peak of the cross-correlation function in each order. We av-

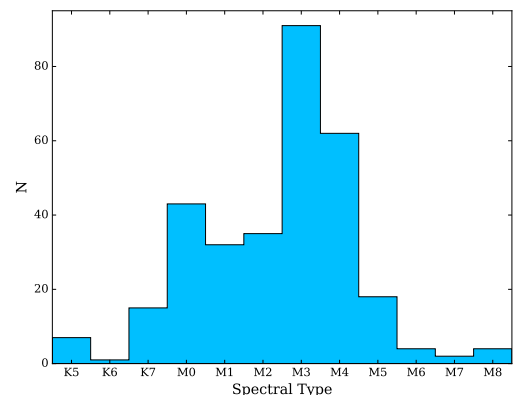


Figure 1. The spectral type distribution of our sample.

erage the radial velocities of all orders to determine a final value, and use the standard deviation of the radial velocity from each order as the measurement uncertainty. All measured radial velocities are given in Table 1. The median uncertainty for our radial velocity measurements is  $\sim 0.7$  km s<sup>-1</sup>. Objects found to be likely spectroscopic binaries via multiple resolved peaks in the

resulting cross-correlations functions are noted in Table 1 and will be discussed further in a future publication.

In Table 2, we combine our radial velocity measurements with astrometry from *Gaia* DR2 (Gaia Collaboration et al. 2018) to calculate full XYZUVW kinematics for each object in our sample. For objects with more than one radial velocity measurement, we take the weighted average. For some objects, astrometry from *Gaia* DR2 was unavailable. In these instances, we filled in astrometry from other sources, as described in the Table 2 astrometry notes.

**Table 2.** Sample Properties

Column Label	Description
2MASS	2MASS Designation
SpT	Spectral Type
SpT_ref	Reference for SpT
Dist	Distance from Gaia DR2
e_Dist	Error in distance
$\mu_\alpha$	Proper motion in right ascension
e_ $\mu_\alpha$	Error in $\mu_\alpha$
$\mu_\delta$	Proper motion in declination
e_ $\mu_\delta$	Error in $\mu_\delta$
ast_note	Astrometry note
RV	Radial velocity
e_RV	Error in radial velocity
X	X position
e_X	Error in X
Y	Y position
e_Y	Error in Y
Z	Z position
e_Z	Error in Z
U	U velocity
e_U	Error in U
V	V velocity
e_V	Error in V
W	W velocity
e_W	Error in W
Gmag	<i>Gaia</i> G magnitude
e_Gmag	Error in Gmag
RPmag	<i>Gaia</i> G <sub>RP</sub> magnitude
e_RPmag	Error in RPmag
BPmag	<i>Gaia</i> G <sub>BP</sub> magnitude

Table 2 continued

**Table 2** (continued)

Column Label	Description
e_BPmag	Error in BPmag
Jmag	2MASS J magnitude
e_Jmag	Error in Jmag
Hmag	2MASS H magnitude
e_Hmag	Error in Hmag
Kmag	2MASS K <sub>S</sub> magnitude
e_Kmag	Error in Kmag
Li	Lithium $\lambda 6707$ equivalent width
H $\alpha$	H $\alpha$ equivalent width
log $L_X$	X-ray luminosity
e_log $L_X$	Error in log $L_X$
FUV	GALEX FUV magnitude
e_FUV	Error in FUV
$f_{FUV}/f_J$	FUV to J flux ratio
NUV	GALEX NUV magnitude
e_NUV	Error in NUV
$f_{NUV}/f_J$	NUV to J flux ratio

NOTE—This table is available in its entirety in a machine-readable form in the online journal.

We searched the literature for previously measured radial velocities for our targets. We found 540 individual radial velocity measurements for 241 of the targets in our sample. Thus, 91 of our targets have radial velocities presented for the first time. In many cases where a previously measured radial velocity is available, our measurement is of significantly higher precision. All previously measured radial velocities are given in Table 3. Excluding spectroscopic binaries noted in Table 1, the median  $\sigma$  difference (difference divided by combined uncertainty) for all previously measured radial velocities compared to our measurements is  $2.45\sigma$ . Note that cases with large radial velocity differences may not necessarily indicate an erroneous measurement, as they could instead be evidence of spectroscopic binarity.

Three catalogs constituted more than half of the previously reported radial velocities of our targets; Malo et al. (2014), the 5th data release of the Radial Velocity Experiment (RAVE; Kunder et al. 2017), and *Gaia* DR2 (Gaia Collaboration et al. 2018). The number of objects in common with *Gaia* DR2 are 99, with a median difference of  $2.06\sigma$ . The number of objects that also have radial velocities in RAVE is 93, with a median difference of  $3.91\sigma$ . The number of objects in common with Malo

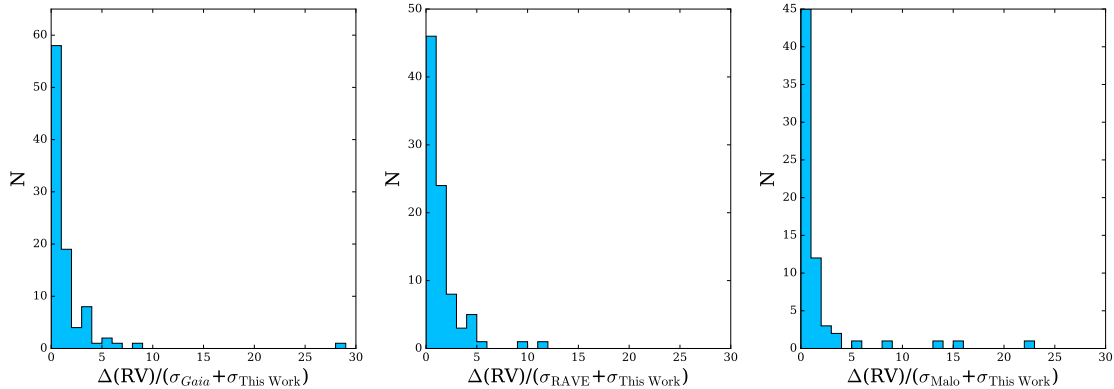


**Figure 2.** Comparison of radial velocities from this work with those determined for the same stars from *Gaia* DR2 (left), RAVE (center) and Malo et al. (2014) (right). The abscissa corresponds to the absolute difference between radial velocity measurements divided by the combined uncertainties for those measurements. Objects noted as spectroscopic binaries in Table 1 are not included in this figure.

et al. (2014) is 74, with a median difference of  $0.58\sigma$ . A comparison of our measured radial velocities with those from *Gaia* DR2, RAVE, and Malo et al. (2014) is shown in Figure 2. The median radial velocity uncertainties for *Gaia* DR2, RAVE, and Malo et al. (2014) measurements are  $1.8 \text{ km s}^{-1}$ ,  $3.9 \text{ km s}^{-1}$ , and  $0.5 \text{ km s}^{-1}$ , respectively.

### 3.3. Age Diagnostics

For each object in our sample, we measure  $\text{H}\alpha$  and Li  $\lambda 6707$  equivalent widths and report the values in Table 2. The detection limit for Li equivalent widths is taken to be  $0.05 \text{ \AA}$  following Shkolnik et al. (2009). Because we aimed for the S/N for each observed spectrum, and the resolutions are similar for each spectrograph, this limit applies to all observations. We also gathered X-ray data from ROSAT (Truemper 1982) using the Second ROSAT all-sky survey (2RXS; Boller et al. 2016). Each detection was converted to an X-ray flux using equations (5) and (6) from Riaz et al. (2006), which was then converted to an X-ray luminosity with the following equation:

$$L_X = 1.2^{38} f_X d^2 \quad (1)$$

which comes from NASA’s High Energy Astrophysics Science Archive Research Center (HEASARC)<sup>1</sup>.

We also include FUV and NUV photometry from the *Galaxy Evolution Explorer* (GALEX), as young ( $<300$  Myr) moving group members have been shown to have higher UV flux levels than field objects in the same mass range (e.g., Rodriguez et al. 2011, Shkolnik et al. 2011, Schneider & Shkolnik 2018).

We also provide *Gaia* DR2 photometry for the entire sample in Table 2, which is used to construct color-

magnitude diagrams in subsequent sections. 2MASS JHK photometry is also provided for convenience.

## 4. DISCUSSION

### 4.1. Objects with Ongoing Accretion

Strong  $\text{H}\alpha$  emission can signify ongoing accretion on low-mass stars. We identify objects that are potentially accreting using the empirical accretion boundary for  $\text{H}\alpha$  equivalent widths presented in Barrado y Navascués & Martín (2003). Note that the empirical relation in Barrado y Navascués & Martín (2003) is only applicable for objects with spectral types earlier than M5.5. Figure 3 shows the  $\text{H}\alpha$  measurements for our entire sample sorted by spectral type. Only one object in our sample with a spectral type later than M5.5 shows strong  $\text{H}\alpha$  absorption ( $\geq -20 \text{ \AA}$ ), the well known flare star DG Phe. Five objects are noted to be above the accretion boundary in the spectral type range K5 to M5.5. However, previous work has shown that the boundary defined in Barrado y Navascués & Martín (2003) does not exclusively identify accretors, as several well known non-accreting flare stars lie above the curve (Shkolnik et al. 2009). Therefore, for any object lying above the Barrado y Navascués & Martín (2003) boundary, we also evaluate the 10%-width defined in White & Basri (2003), which has been shown to better identify accreting objects. White & Basri (2003) define an accretion boundary for the 10%-width of  $>200 \text{ km s}^{-1}$  for non-optically veiled stars.

Of the five objects above the Barrado y Navascués & Martín (2003) curve, one object is the known accretor and  $\beta$  Pic member V4046 Sgr (2MASS J18141047–3247344), with a spectral type of K5+K7 for which we measure a 10%-width of  $447 \text{ km s}^{-1}$ . 2MASS 05082729–2101444 is a second  $\beta$  Pic member, confirmed in Section 4.2.3, with a 10%-width of  $197 \text{ km s}^{-1}$ .

<sup>1</sup> <https://heasarc.gsfc.nasa.gov/W3Browse/all/rassdsstar.html>



**Table 3.** RV Comparisons

2MASS	RV <sub>This Work</sub>	RV <sub>Lit</sub>	Ref
Name	(km s <sup>-1</sup> )	(km s <sup>-1</sup> )	
00153670–2946003	0.61±1.31	63.4	7
...	0.61±1.31	0.02±4.84	61
00213729–4605331	-19.32±0.12	49.2	7
...	-19.32±0.12	-30.70±0.32	24
00501079–0337532	0.27±1.24	5.16±2.98	61
...	0.27±1.24	5.95±4.46	64
00503319+2449009	5.69±0.35	9.2	6
...	5.69±0.35	6.2	15
...	5.69±0.35	6.00±1.10	23
...	5.69±0.35	6.40±11.50	22
...	5.69±0.35	5.60±1.00	16

**References**—(1) Wilson (1967); (2) Woolley et al. (1970); (3) Ochsenbein (1980); (4) Andersen et al. (1985); (5) Gliese & Jahreiß (1991); (6) Reid et al. (1995); (7) Hawley et al. (1996); (8) Uppgren & Harlow (1996); (9) Covino et al. (1997); (10) Thackrah et al. (1997); (11) Delfosse et al. (1998); (12) Strassmeier et al. (2000); (13) Torres et al. (2000); (14) Montes et al. (2001); (15) Gizis et al. (2002); (16) Mochacki et al. (2002); (17) Song et al. (2002); (18) Massey, & Olsen (2003); (19) Nordström et al. (2004); (20) Bochanski et al. (2005); (21) Scholz et al. (2005); (22) Bobylev et al. (2006); (23) Gontcharov (2006); (24) Torres et al. (2006); (25) Blake et al. (2007); (26) Guenther et al. (2007); (27) Kharchenko et al. (2007); (28) Fernández et al. (2008); (29) West et al. (2008); (30) Huélamo et al. (2009); (31) Lépine, & Simon (2009); (32) Reiners, & Basri (2009); (33) Blake et al. (2010); (34) Maldonado et al. (2010); (35) Seifahrt et al. (2010); (36) Kiss et al. (2011); (37) Rodriguez et al. (2011); (38) West et al. (2011); (39) Chubak et al. (2012); (40) Deshpande et al. (2012); (41) Sacco et al. (2012); (42) Malo et al. (2013); (43) Moór et al. (2013); (44) Binks & Jeffries (2014); (45) Elliott et al. (2014); (46) Malo et al. (2014); (47) Newton et al. (2014); (48) Burgasser et al. (2015); (49) Desidera et al. (2015); (50) Guo et al. (2015); (51) Luo et al. (2015); (52) Terrien et al. (2015a); (53) Terrien et al. (2015b); (54) West et al. (2015); (55) Zhong et al. (2015); (56) Binks, & Jeffries (2016); (57) Brewer et al. (2016); (58) Faherty et al. (2016); (59) Luo et al. (2016); (60) Sperauskas et al. (2016); (61) Kunder et al. (2017); (62) Riedel et al. (2017); (63) Frasca et al. (2018); (64) Gaia Collaboration et al. (2018); (65) Reiners et al. (2018)

NOTE—Table 3 is available in its entirety in a machine-readable form in the online journal. A portion is shown here for guidance regarding its form and content.

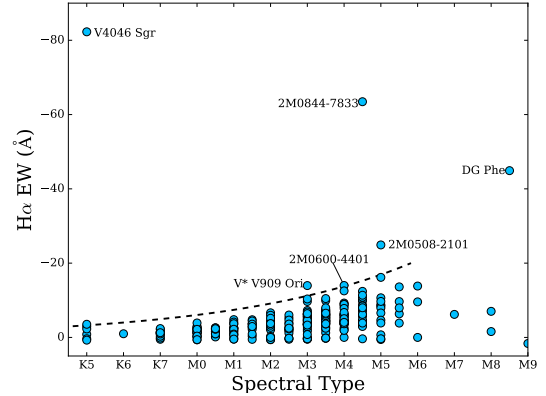


**Figure 3.** H $\alpha$  equivalent width versus spectral type for our entire sample. The dashed line represents the empirical accretor/non-accretor boundary defined in Barrado y Navascués & Martín (2003). All objects on the accretor side of the boundary are labeled and discussed further in the text.

s<sup>-1</sup>, right at the White & Basri (2003) accretion boundary. 2MASS 05425587–0718382 (aka V\* V909 Ori) is another well-known flare star just beyond the accretion boundary in Figure 3, and with a 10%-width of 241 km s<sup>-1</sup>, is likely accreting. This object is rejected as a potential Columba member in Section 4.2.6., though is likely young based on its position in color-magnitude diagrams and its H $\alpha$  emission. 2MASS 08440914-7833457 is a member of the  $\sim$ 11 Myr old  $\eta$  Cha cluster in Section 4.2.8, and is accreting, with a 10%-width of 212 km s<sup>-1</sup>. 2MASS 06002304–4401217 is an object reclassified as a  $\sim$ 45 Myr old member of the Tucana-Horologium Association (see Section 4.2.10), though has a 10%-width of only 121 km s<sup>-1</sup>, and is thus not likely to be accreting.

#### 4.2. Co-Moving Companions

Co-moving systems are valuable benchmarks for testing formation and evolutionary models because the objects in such systems share many of the same physical parameters, such as age, distance, and composition. The astrometric data from *Gaia DR2* allows for a search for co-moving companions to each object in our sample. For each object, we chose a search radius corresponding to 0.1 pc separation at the object’s distance. This separation corresponds to a  $>50\%$  survivability rate according to Weinberg et al. (1987). However, we note that co-moving systems with much larger separations are known to exist (e.g., Oh et al. 2017) and thus our search radius can be thought of as conservative. The average distance for objects in our sample is  $\sim$ 34 pc, which would correspond to a search radius of  $\sim$ 10’. Using the appropriate search radii, we investigated for objects with parallaxes within 0.1 pc of each object in our sample.

To ensure objects are co-moving, we first verify that any potential companions have similar parallaxes by requiring  $\Delta D - 3\sigma_D < 1$  pc (e.g., [Hollands et al. 2018](#)), where  $\Delta D$  is the difference between measured distances, and  $\sigma_D$  is the combined distance uncertainty for the target and potential companion. We then ensure similar proper motions by requiring  $\Delta\mu/\mu < 0.21$ , where  $\Delta\mu \equiv (\Delta\mu_\alpha + \Delta\mu_\delta)^{\frac{1}{2}}$  (e.g., [Dupuy & Liu 2012](#)). Note that this proper motion condition for companionship is valid for proper motions greater than  $\sim 150$  mas yr<sup>-1</sup>. We relax this condition to  $\Delta\mu/\mu < 0.31$  for smaller proper motions. Only two systems required this lower proper motion threshold (systems 9 and 29 in Table 4).

A total of 69 co-moving systems were found, and are listed in Table 4. Systems containing multiple objects in our target list are only listed once. Sixty-three of the sixty-nine systems contain a single co-moving companion, while the remaining 6 systems contain 3 or more components. Figure 4 shows color-magnitude diagrams (CMDs) of all companions using *Gaia* DR2 parallaxes and photometry. The panels show G, G<sub>BP</sub>, and G<sub>RP</sub> photometry ( $\lambda_0 = 673, 532, \text{ and } 797$  nm, respectively; [Jordi et al. 2010](#)). The figure shows that the spectral types of the companions found to objects in our sample are a mix of earlier and later spectral types, along with a handful of white dwarfs.

**Table 4.** Co-Moving Systems

Sys. No.	Comp. No.	Gaia R.A. (°)	Gaia Dec. (°)	plx (mas)	$\mu_\delta$ (mas yr <sup>-1</sup> )	$\mu_\alpha$ (mas yr <sup>-1</sup> )	Separation (")	Separation (AU)
1	1.1	6.45495504961	45.025376915	15.8615±0.0801	102.891±0.08	-9.526±0.036	...	...
...	1.2	6.45743133884	45.0269135029	16.0416±0.1055	102.809±0.111	-8.653±0.05	8.4	523
2	2.1	14.024420588	41.891185381	16.331±0.0607	-78.979±0.103	4.156±0.105	...	...
...	2.2	14.019747768	41.8900123923	15.9529±0.0489	-83.873±0.066	3.93±0.081	13.2	828
3	3.1	15.8126716282	20.0984581507	62.1±0.2033	677.548±0.436	26.765±0.296	...	...
...	3.2	15.812059101	20.0980757415	62.627±0.0425	672.249±0.079	50.851±0.067	2.5	40
4	4.1	18.3735917791	-7.63608776673	15.3648±0.0516	74.651±0.075	-68.292±0.06	...	...
...	4.2	18.3729635322	-7.63663544495	15.6057±0.1904	70.301±0.259	-66.398±0.207	3.0	191
5	5.1	20.2718431581	-4.03570030568	11.1213±0.0475	169.306±0.085	-8.59±0.053	...	...
...	5.2	20.2727145599	-4.03661690337	10.9178±0.0791	171.761±0.148	-8.094±0.074	4.5	417
6	6.1	27.1710820305	-48.5146518446	25.5403±0.0235	110.899±0.037	-53.968±0.036	...	...
...	6.2	27.1995848064	-48.5212175903	25.6167±0.0416	110.54±0.058	-53.667±0.061	72.0	2809
7	7.1	33.4650594831	-41.491991267	11.9977±0.0246	56.572±0.03	-18.784±0.035	...	...
...	7.2	33.4655848276	-41.4911563705	11.9931±0.0188	54.584±0.023	-19.257±0.027	3.3	277
8	8.1	34.2288032428	-23.3703726789	13.7216±0.0778	26.234±0.146	1.122±0.14	...	...
...	8.2	34.2278548085	-23.369533735	13.6387±0.0468	21.64±0.09	-0.189±0.083	4.4	319
9	9.1	37.306737751	-10.1615812986	16.3434±0.076	-34.882±0.106	-18.49±0.105	...	...
...	9.2	37.3065913493	-10.1620032446	16.7055±0.0835	-25.918±0.131	-10.12±0.117	1.6	96
10	10.1	40.3298322728	-57.4217128511	11.3641±0.0451	14.729±0.072	29.64±0.081	...	...
...	10.2	40.3290993909	-57.4215856312	11.6443±0.0783	17.917±0.103	30.519±0.132	1.5	128
11	11.1	41.0893497836	10.9611708044	20.5066±0.1372	67.385±0.285	-56.036±0.242	...	...
...	11.2	41.0950166414	10.9594993429	21.3227±0.0865	73.847±0.178	-58.413±0.146	20.9	981
12	12.1	43.718796959	-7.15734233716	21.5234±0.0666	38.938±0.149	-55.285±0.13	...	...
...	12.2	43.7176761993	-7.15704206394	21.3807±0.0896	34.261±0.194	-64.692±0.165	4.1	194
13	13.1	51.0280110852	23.7845173999	48.2954±0.0494	215.05±0.1	-120.236±0.07	...	...
...	13.2	51.0277404632	23.7851922099	48.0921±0.0617	200.851±0.127	-114.325±0.089	2.6	54

*Table 4 continued*



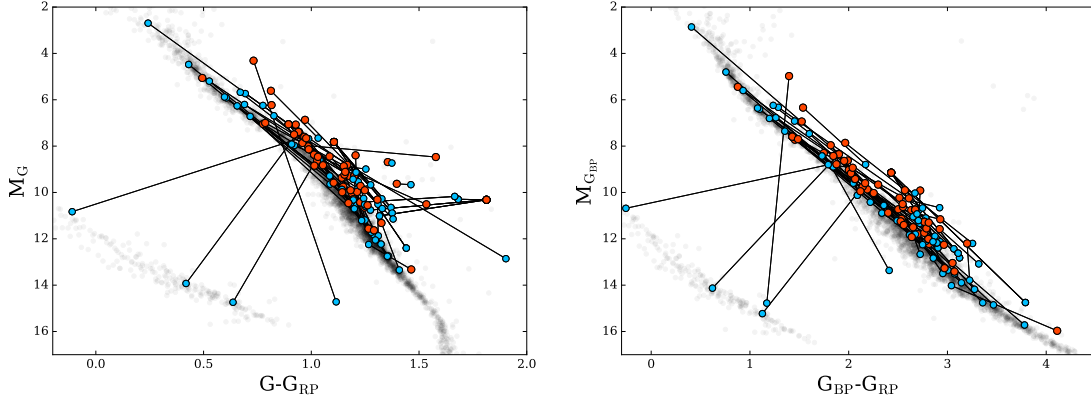


**Figure 4.** *Gaia* CMDs of all co-moving systems found in this work. Objects in our sample are displayed in red, while companions are light blue. For reference, we show all objects from *Gaia* DR2 within 25 pc as background gray symbols.

**Table 4** (*continued*)

Sys. No.	Comp. No.	Gaia R.A. (°)	Gaia Dec. (°)	plx (mas)	$\mu_\delta$ (mas yr <sup>-1</sup> )	$\mu_\alpha$ (mas yr <sup>-1</sup> )	Separation (″)	Separation (AU)
...	13.3	51.0545524391	23.7714861393	48.4516±0.0677	205.518±0.104	-110.346±0.08	99.2	2048
14	14.1	53.0148285759	-51.6652419697	13.0328±0.0228	50.184±0.039	7.261±0.049	...	...
...	14.2	53.016112676	-51.6656193486	13.0197±0.0449	50.644±0.079	6.542±0.097	3.2	244
15	15.1	54.9491321525	33.4751835323	25.465±0.119	-38.631±0.135	-3.727±0.109	...	...
...	15.2	54.9538270286	33.4734135346	25.4853±0.0849	-35.974±0.111	-2.512±0.083	15.5	607
16	16.1	64.4876758851	-38.4513485042	25.5609±0.5218	-95.676±1.166	-64.997±1.007	...	...
...	16.2	64.4923466117	-38.4293196842	26.5906±0.0688	-100.751±0.111	-67.663±0.142	80.4	3023
17	17.1	71.0441624381	-70.323716455	47.5062±0.0253	-120.466±0.046	-65.845±0.055	...	...
...	17.2	71.0450943035	-70.3243619533	47.4314±0.0646	-102.042±0.149	-46.054±0.195	2.6	54
18	18.1	77.5207049404	-23.6709966491	17.3479±0.0408	38.099±0.06	-9.074±0.062	...	...
...	18.2	77.5202711962	-23.6706992996	17.275±0.0487	36.988±0.073	-13.443±0.071	1.8	103
19	19.1	78.2567403265	-70.4607095853	30.9077±0.0738	107.157±0.157	234.762±0.191	...	...
...	19.2	78.257702683	-70.4603692812	31.0644±0.0557	119.442±0.125	223.431±0.113	1.7	54
20	20.1	78.6142599655	-15.247715066	13.145±0.0414	34.552±0.06	-15.176±0.07	...	...
...	20.2	78.6134888585	-15.2477399307	13.1076±0.0653	35.722±0.096	-13.416±0.109	2.7	204
...	20.3	78.6201038834	-15.2485743739	13.1976±0.0467	33.49±0.068	-15.008±0.079	20.5	1556
21	21.1	79.9874389463	-11.4123560204	14.1972±0.0438	27.299±0.07	-21.627±0.069	...	...
...	21.2	79.982721039	-11.4159132296	14.4424±0.0627	26.531±0.097	-22.415±0.093	21.0	1454
22	22.1	87.5469822497	9.66803304279	39.7713±0.182	257.061±0.275	239.913±0.21	...	...
...	22.2	87.55008623	9.66473068132	39.6816±0.1052	263.405±0.142	239.802±0.116	16.2	408
23	23.1	90.0958524601	-44.0225800557	14.4695±0.0525	25.378±0.086	15.806±0.097	...	...
...	23.2	90.0965597837	-44.0227244432	14.4132±0.0538	23.151±0.087	15.075±0.113	1.9	132
24	24.1	91.5725680245	-27.9012654117	27.9688±0.0376	-10.53±0.062	32.007±0.078	...	...
...	24.2	91.5691507809	-27.9056805417	27.9831±0.0294	-16.297±0.039	34.359±0.045	19.3	688
25	25.1	93.4239587636	-28.2545771594	24.2785±0.31	27.198±0.576	86.668±0.516	...	...
...	25.2	93.4239732732	-28.2542821755	23.3908±0.2541	31.168±0.488	90.478±0.491	1.1	45

*Table 4 continued*

Table 4 (continued)

Sys.	Comp.	Gaia R.A.	Gaia Dec.	plx	$\mu_\delta$	$\mu_\alpha$	Separation	Separation
No.	No.	( $^\circ$ )	( $^\circ$ )	(mas)	(mas yr $^{-1}$ )	(mas yr $^{-1}$ )	( $''$ )	(AU)
...	25.3	93.506342479	-28.2611592687	23.606 $\pm$ 0.0791	27.352 $\pm$ 0.11	90.76 $\pm$ 0.128	262.3	11112
...	25.4	93.5068390109	-28.2606529165	23.8732 $\pm$ 0.0426	26.88 $\pm$ 0.059	92.051 $\pm$ 0.069	263.7	11047
26	26.1	93.4385067821	-23.8614582851	59.7617 $\pm$ 0.0243	-47.733 $\pm$ 0.026	110.9 $\pm$ 0.042	...	...
...	26.2	93.4464230422	-23.9064161051	60.0064 $\pm$ 0.0432	-31.043 $\pm$ 0.05	110.803 $\pm$ 0.07	163.9	2732
27	27.1	98.8201005228	-19.1919537555	8.2974 $\pm$ 0.0336	-10.615 $\pm$ 0.05	-28.548 $\pm$ 0.064	...	...
...	27.2	98.8200891154	-19.1923472134	8.2239 $\pm$ 0.0418	-8.326 $\pm$ 0.067	-26.52 $\pm$ 0.066	1.4	172
28	28.1	99.5012976895	-40.9331925133	25.9455 $\pm$ 0.0339	-0.901 $\pm$ 0.072	100.528 $\pm$ 0.064	...	...
...	28.2	99.4934539826	-40.9322052962	25.9428 $\pm$ 0.0551	1.569 $\pm$ 0.106	102.576 $\pm$ 0.101	21.6	834
29	29.1	107.99652442	-35.1711642829	27.0922 $\pm$ 0.0767	-18.251 $\pm$ 0.197	-59.482 $\pm$ 0.158	...	...
...	29.2	107.996305062	-35.1713921997	27.3922 $\pm$ 0.5966	-34.898 $\pm$ 0.937	-50.518 $\pm$ 1.01	1.0	38
30	30.1	122.46684401	3.01931596993	10.2325 $\pm$ 0.0356	-15.159 $\pm$ 0.064	-39.245 $\pm$ 0.04	...	...
...	30.2	122.467210115	3.01985424758	10.2347 $\pm$ 0.0379	-17.262 $\pm$ 0.065	-39.799 $\pm$ 0.042	2.3	229
...	30.3	122.474103517	3.01885247148	10.3936 $\pm$ 0.0544	-16.952 $\pm$ 0.099	-37.131 $\pm$ 0.063	26.2	2516
31	31.1	124.747394623	-72.6653660338	12.3669 $\pm$ 0.0194	-22.13 $\pm$ 0.034	53.681 $\pm$ 0.037	...	...
...	31.2	124.558006465	-72.6262036884	12.4117 $\pm$ 0.0409	-21.677 $\pm$ 0.073	53.863 $\pm$ 0.083	247.5	19937
32	32.1	125.694579057	-57.4459684881	77.4877 $\pm$ 0.0716	-372.239 $\pm$ 0.157	481.326 $\pm$ 0.157	...	...
...	32.2	125.696502898	-57.443984652	77.4495 $\pm$ 0.0706	-371.155 $\pm$ 0.165	437.05 $\pm$ 0.158	8.1	104
33	33.1	127.026873626	-30.6754567721	6.9508 $\pm$ 0.7706	-31.647 $\pm$ 1.355	10.77 $\pm$ 1.414	...	...
...	33.2	127.029755867	-30.6949199474	7.5778 $\pm$ 0.0336	-31.421 $\pm$ 0.042	7.343 $\pm$ 0.048	70.6	9321
34	34.1	130.35521572	-57.6006901021	13.8219 $\pm$ 0.0586	-22.963 $\pm$ 0.13	22.945 $\pm$ 0.116	...	...
...	34.2	130.355051694	-57.6002910335	13.776 $\pm$ 0.071	-29.457 $\pm$ 0.139	22.859 $\pm$ 0.136	1.5	107
35	35.1	133.075291641	-19.2211391051	21.6057 $\pm$ 0.0511	-60.649 $\pm$ 0.071	50.531 $\pm$ 0.058	...	...
...	35.2	133.062595689	-19.2473920359	21.3902 $\pm$ 0.2603	-59.27 $\pm$ 0.256	49.141 $\pm$ 0.299	103.9	4857
36	36.1	133.186640696	22.5149166382	30.533 $\pm$ 0.1048	-40.493 $\pm$ 0.158	-153.386 $\pm$ 0.1	...	...
...	36.2	133.185905577	22.5138295121	30.6652 $\pm$ 0.1024	-36.737 $\pm$ 0.155	-149.973 $\pm$ 0.096	4.6	150
37	37.1	134.972160736	-20.9080635285	16.9812 $\pm$ 0.0342	35.261 $\pm$ 0.055	-72.393 $\pm$ 0.049	...	...
...	37.2	134.977646101	-20.9081030456	16.7952 $\pm$ 0.0895	33.204 $\pm$ 0.155	-72.638 $\pm$ 0.139	18.4	1098
38	38.1	136.022677642	-15.9219506654	36.6103 $\pm$ 0.0483	-109.034 $\pm$ 0.072	-32.638 $\pm$ 0.076	...	...
...	38.2	136.085742643	-15.9143826651	36.52 $\pm$ 0.0517	-107.828 $\pm$ 0.083	-30.936 $\pm$ 0.079	220.0	6025
39	39.1	138.148246805	-15.2844999181	22.0586 $\pm$ 0.0493	-51.328 $\pm$ 0.068	-42.01 $\pm$ 0.093	...	...
...	39.2	138.140600035	-15.2900770922	21.9064 $\pm$ 0.0545	-51.798 $\pm$ 0.088	-43.857 $\pm$ 0.111	33.3	1520
40	40.1	139.691670049	26.7515403197	40.3161 $\pm$ 0.0716	-196.741 $\pm$ 0.102	-353.518 $\pm$ 0.072	...	...
...	40.2	139.671646501	26.7630015702	40.2542 $\pm$ 0.1079	-194.238 $\pm$ 0.15	-353.18 $\pm$ 0.108	76.5	1899
41	41.1	145.658280011	-62.4837073856	23.5547 $\pm$ 0.0847	-149.056 $\pm$ 0.173	83.372 $\pm$ 0.168	...	...
...	41.2	145.657482461	-62.4837573699	23.9316 $\pm$ 0.0425	-158.669 $\pm$ 0.08	73.762 $\pm$ 0.114	1.3	56
...	41.3	145.645472032	-62.4758856653	23.9434 $\pm$ 0.0238	-157.239 $\pm$ 0.045	79.715 $\pm$ 0.044	35.3	1475
42	42.1	153.089944124	-1.47119090641	25.1246 $\pm$ 0.0727	-117.944 $\pm$ 0.147	-10.212 $\pm$ 0.207	...	...
...	42.2	153.08918359	-1.47086683642	25.1079 $\pm$ 0.0777	-112.706 $\pm$ 0.189	1.903 $\pm$ 0.268	3.0	118
43	43.1	154.555865125	-20.4775953826	39.4836 $\pm$ 0.087	-396.396 $\pm$ 0.135	114.239 $\pm$ 0.122	...	...
...	43.2	154.548627208	-20.4720560377	39.3106 $\pm$ 0.0789	-390.304 $\pm$ 0.132	116.753 $\pm$ 0.112	31.5	802

Table 4 continued

Table 4 (continued)

Sys.	Comp.	Gaia R.A.	Gaia Dec.	plx	$\mu_\delta$	$\mu_\alpha$	Separation	Separation
No.	No.	( $^\circ$ )	( $^\circ$ )	(mas)	(mas yr $^{-1}$ )	(mas yr $^{-1}$ )	( $''$ )	(AU)
44	44.1	155.518050963	-32.5575877603	8.2821±0.031	-120.028±0.053	-23.291±0.056	...	...
...	44.2	155.5142724	-32.5585139454	7.2181±0.7932	-120.84±1.348	-23.821±1.464	11.9	1654
45	45.1	156.355439692	-49.3105816883	39.1202±0.0508	-205.315±0.083	61.405±0.07	...	...
...	45.2	156.359926909	-49.3041217036	39.1902±0.0416	-201.765±0.068	68.964±0.057	25.5	651
46	46.1	179.956109675	-42.7405704848	16.1778±0.2008	-72.299±0.253	-16.576±0.201	...	...
...	46.2	179.970249869	-42.733752644	16.1329±0.0866	-73.037±0.105	-18.987±0.072	44.7	2772
47	47.1	182.970867544	12.8202838136	16.3878±0.0793	-71.618±0.13	-57.639±0.074	...	...
...	47.2	182.970853152	12.8199660561	16.1273±0.0976	-74.267±0.18	-63.983±0.092	1.1	71
...	47.3	183.035094024	12.8011015213	16.4079±0.0451	-73.195±0.071	-60.992±0.044	235.8	14371
48	48.1	186.683308106	-12.4884892808	33.3095±0.078	-161.876±0.148	-73.467±0.099	...	...
...	48.2	186.682789758	-12.4886743198	32.6332±0.079	-170.942±0.171	-89.395±0.101	1.9	59
49	49.1	203.881093361	-62.1871496784	4.6833±0.2095	-22.922±0.226	-12.044±0.277	...	...
...	49.2	203.860170132	-62.1851102716	4.0776±1.5383	-18.962±2.782	-11.943±3.049	35.9	8805
50	50.1	207.68317614	-21.6924529707	47.4932±0.0596	-35.895±0.113	-377.302±0.102	...	...
...	50.2	207.598875406	-21.6238049614	47.5095±0.0663	-33.504±0.111	-376.208±0.11	375.0	7893
51	51.1	220.495473154	-16.8880611197	46.683±0.0522	-170.941±0.093	-247.728±0.081	...	...
...	51.2	220.494457166	-16.8179334119	46.6443±0.0757	-171.652±0.125	-247.082±0.11	252.5	5413
52	52.1	220.908135379	-4.24352280153	19.3726±0.1992	-101.846±0.294	-69.609±0.275	...	...
...	52.2	220.907855485	-4.2434345354	19.4511±0.1454	-112.583±0.229	-66.234±0.203	1.1	54
53	53.1	237.528545136	-45.4227023254	21.3324±0.0492	32.526±0.109	-33.392±0.079	...	...
...	53.2	237.568220468	-45.4018597943	21.3601±0.0533	39.755±0.129	-33.474±0.068	125.2	5863
54	54.1	254.334352878	-53.7258072971	19.7563±0.12	-10.849±0.187	-84.087±0.143	...	...
...	54.2	254.339199055	-53.7247727621	19.8171±0.1371	-16.204±0.156	-85.696±0.138	11.0	554
55	55.1	261.990267808	-40.2737800294	24.9806±0.0702	-22.095±0.134	-61.126±0.094	...	...
...	55.2	261.989622771	-40.2736500924	25.025±0.065	-16.192±0.123	-58.788±0.087	1.8	73
56	56.1	272.81636071	-78.9886459065	85.2009±0.3832	97.719±0.717	275.387±0.759	...	...
...	56.2	272.814906041	-78.9883766915	85.8373±0.3909	60.499±0.728	304.053±0.745	1.4	16
57	57.1	273.543692455	-32.7931482752	13.8111±0.0642	3.491±0.111	-52.754±0.087	...	...
...	57.2	273.591990323	-32.7697082458	13.9995±0.0521	3.081±0.101	-52.639±0.08	168.8	12057
58	58.1	279.909851791	16.3866196343	14.3647±0.0404	-20.777±0.06	-106.458±0.072	...	...
...	58.2	279.899837715	16.3820506469	14.515±0.1599	-19.859±0.267	-107.222±0.33	38.3	2639
59	59.1	294.287243177	-51.5670290492	20.4834±0.0421	91.125±0.068	-26.99±0.048	...	...
...	59.2	294.284544043	-51.5687325295	20.4788±0.0579	87.338±0.085	-23.971±0.06	8.6	420
60	60.1	295.853742242	-37.3705104884	41.264±0.0648	162.885±0.098	-183.23±0.062	...	...
...	60.2	295.853258439	-37.3702613909	44.321±0.3694	155.208±0.539	-182.811±0.387	1.6	37
61	61.1	320.370809461	-66.9188363806	31.7121±0.3965	105.13±0.671	-85.324±0.782	...	...
...	61.2	320.353108276	-66.9163705624	31.2692±0.0434	95.668±0.062	-100.258±0.081	26.5	848
62	62.1	326.832200245	-48.0550277575	15.7704±0.1229	54.193±0.151	-89.707±0.215	...	...
...	62.2	326.816594573	-48.0445477226	15.9461±0.0552	49.848±0.07	-84.906±0.096	53.2	3338
63	63.1	332.922938405	-20.7366560482	24.1987±0.0867	147.272±0.138	-61.669±0.122	...	...

Table 4 continued

Table 4 (continued)

Sys.	Comp.	Gaia R.A.	Gaia Dec.	plx	$\mu_\delta$	$\mu_\alpha$	Separation	Separation
No.	No.	( $^\circ$ )	( $^\circ$ )	(mas)	(mas yr $^{-1}$ )	(mas yr $^{-1}$ )	( $''$ )	(AU)
...	63.2	332.926084587	-20.7386890403	24.2517 $\pm$ 0.0877	146.754 $\pm$ 0.144	-64.44 $\pm$ 0.126	12.9	531
64	64.1	342.48416723	17.744598513	13.0626 $\pm$ 0.2053	-28.967 $\pm$ 0.378	-64.631 $\pm$ 0.29	...	...
...	64.2	342.480450677	17.7442276081	13.6598 $\pm$ 0.126	-27.113 $\pm$ 0.257	-55.2 $\pm$ 0.178	12.8	938
65	65.1	347.973950223	-45.1338600039	21.1338 $\pm$ 0.1211	74.896 $\pm$ 0.105	-94.183 $\pm$ 0.172	...	...
...	65.2	347.967423785	-45.1366897831	20.8274 $\pm$ 0.0683	87.469 $\pm$ 0.05	-93.499 $\pm$ 0.091	19.5	934
66	66.1	350.19685687	-67.3896567818	24.3611 $\pm$ 0.0738	78.28 $\pm$ 0.12	-81.043 $\pm$ 0.119	...	...
...	66.2	350.197395285	-67.3888825742	24.4343 $\pm$ 0.0656	84.043 $\pm$ 0.104	-78.354 $\pm$ 0.101	2.9	118
67	67.1	351.888430293	-22.0418804446	14.5199 $\pm$ 0.1203	61.6 $\pm$ 0.233	-50.315 $\pm$ 0.173	...	...
...	67.2	351.885024487	-22.0388739146	14.577 $\pm$ 0.0509	60.982 $\pm$ 0.103	-50.158 $\pm$ 0.074	15.7	1077
68	68.1	353.342398779	-12.6685927216	27.809 $\pm$ 0.4086	189.131 $\pm$ 0.549	24.159 $\pm$ 0.49	...	...
...	68.2	353.350093919	-12.664513128	29.4073 $\pm$ 0.064	185.523 $\pm$ 0.091	24.355 $\pm$ 0.078	30.8	1046
69	69.1	358.423396079	-65.9480499764	39.5909 $\pm$ 0.0328	-43.768 $\pm$ 0.047	87.533 $\pm$ 0.047	...	...
...	69.2	358.415716065	-65.9467703123	39.5453 $\pm$ 0.0268	-42.373 $\pm$ 0.039	84.84 $\pm$ 0.044	12.2	308

#### 4.3. Moving Group Membership

We evaluate each object for potential moving group membership using the BANYAN  $\Sigma$  tool (Gagné et al. 2018a), which evaluates the membership probabilities by comparing positions to known members of different groups using a Bayesian classifier. BANYAN  $\Sigma$  considers all kinematic information (position, proper motion, parallax, and radial velocity) to compare 6-dimensional XYZUVW coordinates to known groups using multivariate Gaussians. While we evaluate membership in all groups included in BANYAN  $\Sigma$ , potential matches from our sample were found for 10 groups listed in Table 5. Any object with a BANYAN  $\Sigma$  probability of  $>1\%$  for a particular group was investigated for potential membership. The TW Hya and Scorpius-Centaurus Associations are part of a larger, targeted search for new

members by our research group, and will be discussed in a forthcoming separate study.

Note that a kinematic match to a particular group using BANYAN  $\Sigma$  does not guarantee membership because kinematic interlopers with different ages are possible. For all kinematic matches, we also evaluate membership using all available age information gathered in Table 4 to ensure consistency with the age of any matching group. Note that any objects in our list that are already included in the bonafide members of BANYAN  $\Sigma$  are not discussed further. Table 5 summarizes the number of new, confirmed, and rejected members found for all groups. Table 6 provides age and kinematic information for new, confirmed, and reassigned moving group and association members, while Table 7 provides information for all rejected moving group and association members. Notes for each group including comments on individual sources are presented in the following sections.

**Table 5.** Moving Group Evaluation Summary

Group	Age	Age	New <sup>a</sup>	Confirmed	Rejected
Name	(Myr)	Ref.	Members	Members	Members
AB Dor	$149^{+51}_{-19}$	1	0	13	5
Argus	40-50	2	0	7	21
$\beta$ Pictoris	$22 \pm 6$	3	1	8	10
Carina	$45^{+11}_{-7}$	1	3	8	1
Carina-Near	$\sim 200$	4	6	0	0
Columba	$42^{+6}_{-4}$	1	1	10	5
$\epsilon$ Cha	$3.7^{+4.6}_{-1.4}$	5	0	4	0
$\eta$ Cha	$11 \pm 3$	1	0	8	0
Octans	$35 \pm 5$	6	0	1	0
Tuc-Hor	$45 \pm 4$	1	3	4	2
Total			14	63	46

<sup>a</sup>This number includes those objects that have been previously suggested to be a member of a different group, but have been re-assigned in this work to this group.

**References**—(1) Bell et al. (2015); (2) Zuckerman (2019); (3) Shkolnik et al. (2017); (4) Zuckerman et al. (2006); (5) Murphy et al. (2013); (6) Murphy & Lawson (2015)

Table 6. New and Confirmed Moving Group Members

2MASS Name	Spec. Type	Li EW <sup>a</sup> (Å)	H $\alpha$ EW (Å)	log $L_X$ (erg s <sup>-1</sup> )	$f_{FUV}/f_J$	$f_{NUV}/f_J$	XYZ (pc)	UVW (km s <sup>-1</sup> )	BANYAN $\Sigma$ (%)	New? <sup>a</sup>
AB Dor										
01484087-4830519	M1.5	...	-2.68	29.36±0.07	3.41e-05	2.04e-04	(2.58,-15.78,-35.74)	(-7.51,-28.13,-11.48)	99.8	...
02130073+1803460	M4.5	...	-5.49	...	6.33e-05	2.05e-04	(-17.55,10.62,-17.63)	(-5.33,-27.42,-15.48)	99.9	...
03100305-2341308	M3.5	...	-6.20	...	7.96e-05	2.09e-04	(-11.31,-7.77,-22.49)	(-4.75,-27.53,-16.92)	99.3	...
04084031-2705473	M4.0	...	-3.60	28.92±0.10	8.77e-05	2.13e-04	(-15.80,-15.64,-23.35)	(-5.47,-28.22,-16.53)	99.6	...
04353618-2527347	M3.5	...	-5.80	28.71±0.08	5.37e-05	2.28e-04	(-9.15,-8.98,-10.82)	(-5.10,-28.05,-18.16)	98.4	...
04514615-2400087	M3.0	...	-6.23	29.17±0.09	...	2.24e-04	(-29.39,-28.34,-29.91)	(-4.47,-26.77,-8.52)	65.2	...
05531299-4505119	M0.5	0.132	-1.57	29.23±0.04	1.86e-05	...	(-8.58,-25.99,-15.01)	(-8.05,-28.67,-12.02)	99.9	...
06373215-2823125	M2.5	...	-1.79	29.14±0.10	...	...	(-22.44,-35.02,-11.40)	(-8.13,-27.50,-15.07)	99.9	...
12383713-2703348	M2.5	...	-2.31	28.80±0.10	2.10e-05	1.22e-04	(9.92,-17.60,14.53)	(-7.43,-28.51,-11.92)	99.7	...
14415908-1653133	M3.0	...	0.00	...	1.88e-04	2.11e-04	(15.49,-6.43,13.32)	(-11.76,-25.47,-16.49)	60.2	...
21464282-8543046	M3.5	...	-10.46	28.82±0.05	6.23e-05	...	(8.00,-10.82,-7.78)	(-7.52,-27.45,-13.94)	100.0	...
21471964-4803166	M4.0	...	-6.72	29.32±0.11	4.94e-05	1.76e-04	(41.13,-7.39,-47.70)	(-5.68,-29.52,-14.00)	16.5	...
23115362-4508004	M3.0	...	-6.41	29.81±0.07	6.51e-05	...	(20.51,-5.83,-42.24)	(-4.67,-26.66,-10.46)	84.1	...
Argus										
05471788-2856130	M3.5	...	-5.54	29.64±0.07	...	...	(-33.46,-45.69,-27.42)	(-20.98,-15.20,-4.12)	99.7	...
09445422-1220544	M5.0	...	-16.17	28.71±0.04	3.94e-05	1.25e-04	(-4.28,-10.54,6.56)	(-22.36,-13.61,-3.75)	99.5	...
10252563-4918389	M4.0	...	-4.52	28.86±0.09	...	...	(4.38,-25.00,3.08)	(-24.26,-6.60,-6.75)	5.9	...
12233860-4606203	M4.0	...	-5.08	28.71±0.09	...	1.17e-04	(10.29,-19.42,6.51)	(-24.03,-8.03,-5.63)	89.4	...
17275761-4016243	M4.0	...	-7.81	28.91±0.14	...	...	(39.17,-7.98,-2.12)	(-20.07,-8.15,-1.98)	81.4	...
20072376-5147272	K6.0	...	-0.99	29.79±0.04	4.58e-05	3.75e-04	(27.96,-6.54,-18.30)	(-25.74,-16.72,-5.09)	95.3	...
22274882-0113527	M3.5	...	-3.64	28.98±0.10	9.73e-05	...	(8.95,18.16,-21.66)	(-24.17,-16.59,-0.16)	84.4	...
$\beta$ Pic										
02442137+1057411	M1.0	0.739	-2.63	...	...	...	(-33.95,10.76,-33.31)	(-8.96,-18.36,-5.00)	3.9	...
02490228-1029220	M2.0	0.266	-2.42	29.34±0.20	3.97e-05	1.78e-04	(-20.65,-2.75,-32.97)	(-12.38,-10.28,-11.32)	1.3	...
05082729-2101444	M5.0	...	-24.90	28.89±0.13	2.57e-05	1.53e-04	(-30.78,-27.73,-25.52)	(-14.65,-20.39,-7.73)	2.5	...
05294468-3239141	M4.5	...	-5.88	29.03±0.08	2.27e-05	1.03e-04	(-14.16,-21.49,-15.16)	(-11.90,-16.36,-9.04)	99.9	...
05320450-0305291	M2.0	0.073	-3.02	29.80±0.04	...	1.93e-04	(-29.25,-14.56,-11.27)	(-19.08,-15.64,-8.73)	51.3	...
09462782-4457408	M5.5	0.542	-13.61	...	...	...	(1.60,-46.39,5.29)	(-13.99,-17.17,-7.78)	40.9	Y

Table 6 continued



Table 6 (continued)

2MASS Name	Spec. Type	Li EW <sup>a</sup> (Å)	H $\alpha$ EW (Å)	$\log L_X$ (erg s <sup>-1</sup> )	$f_{FUV}/f_J$	$f_{NUV}/f_J$	XYZ (pc)	UVW (km s <sup>-1</sup> )	BANYAN $\Sigma$ (%)	New? <sup>a</sup>
13545390-7121476	M2.5	...	-2.84	28.86±0.06	...	2.32e-04	(13.89,-17.78,-3.62)	(-12.02,-15.03,-10.41)	99.4	...
16572029-5343316	M3.0	...	-0.78	29.14±0.16	...	...	(45.37,-21.65,-5.88)	(-7.12,-15.99,-10.52)	98.7	...
19233820-4606316	M0.0	0.447	-1.01	29.75±0.11	3.04e-05	3.32e-04	(64.02,-9.10,-29.50)	(-7.02,-16.34,-9.64)	97.0	...
Carina										
061112997-7213388	M4.0	...	-6.16	29.40±0.06	4.56e-05	1.42e-04	(11.12,-48.65,-27.40)	(-11.88,-24.50,-4.88)	97.7	...
06234024-7504327	M3.5	...	-5.65	29.52±0.33	...	...	(11.77,-40.75,-22.48)	(-5.30,-20.45,-6.12)	98.6	...
07013884-6236059	M0.5	...	-1.54	29.70±0.05	9.52e-05	2.66e-04	(4.33,-81.70,-34.29)	(-11.40,-23.04,-4.93)	94.6	Y
07065772-5353463	M0.0	0.380	-1.36	29.66±0.06	4.46e-05	1.83e-04	(-4.32,-43.79,-15.54)	(-10.75,-20.78,-6.24)	96.2	R <sup>c</sup>
08040534-6316396	M2.0	...	-5.17	29.81±0.09	...	...	(8.46,-74.44,-22.07)	(-11.13,-22.50,-6.22)	100.0	...
08194309-7401232	M4.5	...	-9.80	29.49±0.13	...	1.48e-04	(17.96,-58.19,-22.48)	(-9.29,-28.84,-8.53)	82.7	...
08412528-5736021	M3.0	...	-7.24	...	...	...	(5.13,-71.17,-11.93)	(-9.49,-21.70,-5.11)	96.7	...
09032434-6348330	M0.5	0.380	-2.14	29.92±0.08	...	...	(14.38,-75.70,-15.34)	(-10.58,-22.68,-6.44)	100.0	...
09180165-5452332	M4.0	0.285	-8.96	29.25±0.13	...	...	(4.95,-52.65,-3.57)	(-11.61,-26.26,-6.41)	96.9	...
09315840-6209258	M3.5	...	-6.15	29.94±0.09	...	...	(15.90,-76.08,-10.61)	(-10.24,-21.08,-6.19)	99.9	...
14284804-7430205	M1.0	0.099	-2.19	29.66±0.08	...	...	(36.41,-44.30,-13.11)	(-9.25,-20.94,-5.72)	4.2	R <sup>d</sup>
Carina-Near										
06134171-2815173	M3.5	...	-5.93	29.16±0.07	6.09e-05	3.04e-04	(-22.08,-31.75,-14.18)	(-28.32,-16.28,0.85)	9.5	Y
06380031-4056011	M3.5	...	-6.52	28.98±0.09	...	...	(-12.60,-34.01,-13.03)	(-25.58,-18.93,-3.29)	99.7	R <sup>d</sup>
07170438-6311123	M2.0	...	-4.43	29.41±0.07	...	...	(4.43,-60.49,-23.56)	(-13.61,-13.78,-4.57)	1.6	R <sup>f</sup>
11462310-5238519	M4.5	...	-8.46	...	...	3.55e-04	(22.38,-52.65,9.03)	(-19.04,-16.72,-1.61)	45.9	R <sup>b</sup>
19435432-0546363	M4.0	...	-5.65	28.94±0.11	6.12e-05	1.71e-04	(23.53,15.70,-7.21)	(-31.38,-15.13,1.45)	65.3	R <sup>d</sup>
20284361-1128307	M3.5	...	-6.30	28.85±0.07	4.88e-05	1.83e-04	(13.65,8.99,-8.23)	(-23.85,-17.91,-3.00)	70.0	R <sup>e</sup>
Columba										
03241504-5901125	K7.0	0.224	-0.94	29.75±0.10	4.62e-05	3.35e-04	(4.10,-57.06,-65.05)	(-11.03,-22.83,-5.04)	8.2	...
03320347-5139550	M2.0	...	-2.06	29.75±0.07	2.33e-05	1.43e-04	(-5.66,-47.72,-59.82)	(-12.39,-21.79,-3.71)	97.5	...
04091413-4008019	M3.5	...	-6.04	29.59±0.12	3.26e-05	1.90e-04	(-22.59,-45.88,-55.64)	(-12.70,-21.84,-4.39)	99.9	...
05100427-2340407	M3.0	...	-2.20	29.89±0.05	3.69e-05	1.47e-04	(-34.45,-34.58,-30.66)	(-14.04,-22.04,-5.26)	99.9	...
05100488-2340148	M2.0	...	-6.63	...	5.94e-05	2.25e-04	(-34.60,-34.73,-30.79)	(-13.01,-22.52,-5.76)	100.0	...
05175793-5433503	M2.0	...	-5.96	29.72±0.13	...	1.09e-04	(-8.11,-60.00,-42.68)	(-12.16,-22.91,-5.10)	83.4	Y
05195695-1124440	M3.5	...	-9.91	29.65±0.09	...	1.74e-04	(-53.30,-34.72,-30.24)	(-14.30,-21.71,-5.51)	99.2	...
05241317-2104427	M4.0	...	-4.84	29.25±0.11	...	...	(-37.13,-35.27,-27.45)	(-13.62,-21.95,-6.02)	100.0	...
05395494-1307598	M3.0	...	-3.65	29.51±0.13	...	...	(-58.54,-44.11,-29.17)	(-15.50,-22.55,-6.76)	42.7	...

Table 6 continued

Table 6 (continued)

2MASS Name	Spec. Type	Li EW <sup>a</sup> (Å)	H $\alpha$ EW (Å)	$\log L_X$ (erg s <sup>-1</sup> )	$f_{FUV}/f_J$	$f_{NUV}/f_J$	XYZ (pc)	UVW (km s <sup>-1</sup> )	BANYAN $\Sigma$ (%)	New? <sup>a</sup>
05432676-3025129	M0.5	...	-2.60	29.97±0.07	...	...	(-44.52,-63.78,-39.77)	(-14.45,-23.33,-8.36)	1.3	...
06262932-0739540	M1.0	0.228	-2.43	...	...	...	(-64.68,-48.69,-12.84)	(-12.56,-20.72,-6.11)	71.5	...
$\epsilon$ Cha										
11493184-7851011	M0.0	0.579	-2.96	30.07±0.06	8.10e-05	3.25e-04	(48.15,-83.91,-28.38)	(-9.77,-20.95,-11.13)	99.9	...
12194369-7403572	M1.0	0.575	-4.13	...	...	2.03e-04	(50.77,-85.45,-19.92)	(-9.25,-21.01,-9.65)	99.8	...
12202177-7407393	M1.0	0.663	-3.69	...	1.29e-04	1.96e-04	(74.70,-125.45,-29.40)	(-18.45,-24.39,-8.85)	20.9	...
12210499-7116493	K7.0	0.549	-0.93	30.32±0.09	...	...	(49.88,-84.76,-14.79)	(-9.19,-20.65,-8.84)	95.4	...
$\eta$ Cha										
08361072-7908183	M5.5	0.621	-9.65	...	...	...	(34.85,-84.45,-36.82)	(-10.89,-20.99,-11.38)	92.2	...
08385150-7916136	M5.0	0.652	-10.67	...	...	...	(35.83,-86.00,-37.47)	(-10.72,-20.74,-11.49)	38.7	...
08413030-7853064	M5.0	0.685	-8.46	...	...	...	(34.91,-84.97,-36.38)	(-11.89,-20.35,-11.09)	41.6	...
08413703-7903304	M3.5	0.529	-2.63	...	...	...	(35.13,-84.83,-36.52)	(-10.95,-20.58,-10.84)	57.6	...
08422710-7857479	M4.0	0.680	-4.51	...	...	...	(35.04,-84.88,-36.37)	(-11.25,-20.86,-11.57)	38.9	...
08423879-7854427	M3.0	0.487	-4.25	29.00±0.29	...	...	(34.76,-84.37,-36.07)	(-10.68,-20.98,-11.22)	84.9	...
08440914-7833457	M4.5	0.536	-63.46	...	...	...	(34.54,-84.99,-35.81)	(-10.90,-20.35,-11.14)	79.1	...
08441637-7859080	M4.5	0.643	-10.14	...	...	...	(34.63,-83.59,-35.72)	(-11.35,-20.65,-12.92)	99.6	...
Octans										
02411909-5725185	M3.0	...	-4.63	29.57±0.14	2.20e-05	1.71e-04	(7.11,-51.18,-71.23)	(-12.82,-2.56,-8.81)	100.0	...
Tuc-Hor										
00153670-2946003	M4.0	...	-6.32	28.76±0.15	2.32e-05	1.33e-04	(5.15,1.12,-36.09)	(-9.60,-20.98,-2.64)	99.9	...
03454058-7509121	M4.0	...	-8.36	29.34±0.07	...	1.61e-04	(15.69,-42.86,-34.78)	(-9.61,-21.19,-1.00)	100.0	...
05142736-1514514	M3.5	...	-5.42	29.74±0.08	...	...	(-53.96,-39.79,-35.95)	(-13.54,-22.30,-2.33)	20.4	R <sup>c</sup>
05142878-1514546	M3.5	...	-4.53	...	...	...	(-53.75,-39.64,-35.80)	(-13.16,-21.71,-2.39)	24.1	R <sup>c</sup>
06002304-4401217	M4.0	...	-13.98	29.75±0.05	...	...	(-20.16,-58.02,-31.67)	(-11.70,-23.70,-3.12)	59.9	R <sup>c</sup>
19225071-6310581	M3.0	...	-6.21	29.65±0.12	5.47e-05	1.88e-04	(41.60,-21.03,-24.27)	(-8.68,-19.27,-0.01)	97.9	...
23204705-6723209	M5.0	...	-9.69	29.25±0.08	8.26e-05	2.34e-04	(19.83,-19.43,-30.24)	(-8.74,-21.03,-0.55)	99.9	...

Table 6 continued

**Table 6** (*continued*)

2MASS	Spec.	Li EW <sup>a</sup>	H $\alpha$ EW	$\log L_X$	$f_{FUV}/f_J$	$f_{NUV}/f_J$	XYZ	UVW	BANYAN $\Sigma$	New? <sup>a</sup>
Name	Type	( $\text{\AA}$ )	( $\text{\AA}$ )	( $\text{erg s}^{-1}$ )			(pc)	( $\text{km s}^{-1}$ )	(%)	

<sup>a</sup> 'Y' refers to completely new members, while 'R' refers to reassigned members (i.e., those objects previously proposed to belong to a different group).

<sup>b</sup> Previously suggested to be a member of the Scorpius-Centaurus OB association in Rodriguez et al. (2011).

<sup>c</sup> Previously suggested to be a member of the Columba association in Malo et al. (2013, 2014).

<sup>d</sup> Previously suggested to be a member of the Argus association in Malo et al. (2013).

<sup>e</sup> Previously suggested to be a member of the Argus association in Riedel et al. (2014).

<sup>f</sup> Previously suggested as an ambiguous  $\beta$  Pic/Carina/Columba/AB Dor member in Malo et al. (2013)

Table 7. Rejected Moving Group Members

2MASS	Spec.	Li EW <sup>a</sup>	H $\alpha$ EW	$\log L_X$	$f_{FUV}/f_J$	$f_{NUV}/f_J$	XYZ	UVW	Reassigned?
Name	Type	( $\text{\AA}$ )	( $\text{\AA}$ )	( $\text{erg s}^{-1}$ )			(pc)	( $\text{km s}^{-1}$ )	
AB Dor									
02523096-1548357	M2.5	...	-2.35	29.72 $\pm$ 0.17	3.43e-05	1.71e-04	(-54.46,-16.88,-97.76)	(-30.87,-79.45,-54.38)	...
04424932-1452268	M4.0	...	-6.00	29.00 $\pm$ 0.10	...	1.75e-04	(-24.41,-15.55,-20.33)	(-1.67,-30.52,-13.76)	...
05130132-7027418	M3.5	...	-5.11	29.16 $\pm$ 0.04	...	5.45e-05	(5.38,-26.40,-17.91)	(-37.95,-8.56,8.43)	...
05240991-4223054	M0.5	...	-2.41	29.80 $\pm$ 0.09	...	1.84e-04	(-31.89,-77.48,-55.42)	(-11.00,-31.02,-11.84)	...
07115917-3510157	M3.0	...	-4.86	29.11 $\pm$ 0.09	...	...	(-14.27,-33.25,-7.29)	(10.52,4.10,-5.89)	...
Argus									
00503319+2449009A	M3.5	...	-4.18	28.97 $\pm$ 0.06	6.59e-05	1.57e-04	(-6.36,9.92,-9.23)	(-13.79,-5.23,-5.34)	...
00503319+2449009B	M3.5	...	-4.53	...	6.59e-05	1.57e-04	(-6.36,9.92,-9.23)	(-13.76,-5.28,-5.30)	...
03282609-0537361	M4.0	...	-4.32	28.26 $\pm$ 0.18	2.06e-05	9.95e-05	(-18.84,-3.38,-20.48)	(-25.43,-16.13,-12.27)	...
03415581-5542287	M4.5	...	-7.28	...	1.51e-04	1.83e-04	(-0.63,-18.14,-20.31)	(-43.27,-26.49,-9.91)	...
03415608-5542408	M4.0	...	-3.84	28.47 $\pm$ 0.10	...	9.50e-05	(-0.63,-18.14,-20.31)	(-43.04,-19.94,-2.58)	...
04464970-6034109	M1.5	...	-4.42	28.99 $\pm$ 0.05	...	...	(0.13,-19.20,-15.31)	(-14.20,-7.41,-1.88)	...
04595855-0333123	M4.0	...	-5.50	29.46 $\pm$ 0.10	8.52e-05	1.63e-04	(-50.26,-21.13,-26.97)	(-44.90,-19.46,1.19)	...
06380031-4056011	M3.5	...	-6.52	28.98 $\pm$ 0.09	...	...	(-12.60,-34.01,-13.03)	(-25.58,-18.93,-3.29)	Y
07343426-2401353	M3.5	...	-6.19	29.06 $\pm$ 0.13	...	...	(-21.54,-35.95,-1.41)	(-16.88,-18.69,-3.72)	...
09423823-6229028	M3.5	...	-1.24	29.19 $\pm$ 0.10	...	...	(9.44,-41.05,-5.31)	(-30.35,-18.15,-8.55)	...
09455843-3253299	M4.5	...	-8.60	28.41 $\pm$ 0.06	4.01e-05	1.06e-04	(-1.25,-11.51,3.22)	(-21.09,-24.78,2.03)	...
11200609-1029468	M2.0	...	-1.42	29.01 $\pm$ 0.05	1.02e-05	1.08e-04	(-0.14,-13.05,13.68)	(-16.40,-13.75,3.95)	...
13283294-3654233	M3.5	...	-2.47	28.88 $\pm$ 0.13	...	1.20e-04	(21.27,-24.35,15.34)	(-39.22,-8.01,-5.41)	...
13382562-2516466	M3.5	...	-3.73	29.25 $\pm$ 0.07	7.79e-05	2.95e-04	(18.11,-17.40,18.51)	(-59.23,-10.66,-20.64)	...
13591045-1950034	M4.5	...	-4.63	28.33 $\pm$ 0.07	1.66e-05	6.18e-05	(6.68,-4.86,6.99)	(-28.11,-16.99,-9.81)	...
14284804-7430205	M1.0	0.099	-2.19	29.66 $\pm$ 0.08	...	...	(36.41,-44.30,-13.11)	(-9.25,-20.94,-5.72)	Y
19432464-3722108	M3.5	...	-7.41	28.60 $\pm$ 0.13	...	...	(21.79,0.87,-10.56)	(-45.72,-17.12,-3.86)	...
19435432-0546363	M4.0	...	-5.65	28.94 $\pm$ 0.11	6.12e-05	1.71e-04	(23.53,15.70,-7.21)	(-31.38,-15.13,1.45)	Y
20163382-0711456	M0.0	...	-0.35	29.06 $\pm$ 0.09	1.40e-05	1.30e-04	(25.59,18.73,-12.93)	(-23.01,-5.84,5.44)	...
20284361-1128307	M3.5	...	-6.30	28.85 $\pm$ 0.07	4.88e-05	1.83e-04	(13.65,8.99,-8.23)	(-23.85,-17.91,-3.00)	Y
23332198-1240072	K5.0	...	-3.54	28.99 $\pm$ 0.11	5.38e-05	...	(5.46,13.14,-33.03)	(-27.22,-1.99,-25.93)	...
$\beta$ Pic									

Table 7 continued

Table 7 (continued)

2MASS Name	Spec. Type	Li EW <sup>a</sup> (Å)	H $\alpha$ EW (Å)	$\log L_X$ (erg s <sup>-1</sup> )	$f_{FUV}/f_J$	$f_{NUV}/f_J$	XYZ (pc)	UVW (km s <sup>-1</sup> )	Reassigned?
05332802-4257205	M4.5	...	-2.95	28.43±0.04	2.77e-05	9.80e-05	(-3.21,-8.18,-5.46)	(-0.30,4.85,2.09)	...
05422387-2758031	M4.5	...	-8.50	29.57±0.08	9.63e-05	2.28e-04	(-36.00,-46.73,-29.48)	(-4.12,-9.55,-5.49)	...
06135773-2723550	G5.0	0.076	-5.55	31.16±0.07	7.67e-05	7.72e-04	(-204.69,-285.40,-126.33)	(1.59,13.84,9.77)	...
08224744-5726530	M4.5	...	-6.09	28.34±0.05	...	...	(0.56,-12.64,-2.56)	(-36.48,-15.61,-5.83)	...
10571139+0544547	M1.0	...	-1.33	30.09±0.09	5.67e-05	2.81e-04	(-24.25,-54.39,86.41)	(-18.97,-29.34,-10.74)	...
11493184-7851011	M0.0	0.579	-2.96	30.07±0.06	8.10e-05	3.25e-04	(48.15,-83.91,-28.38)	(-9.77,-20.95,-11.13)	Y
12115308+1249135	M0.0	...	-0.14	...	1.73e-05	1.37e-04	(-0.60,-17.87,58.34)	(-9.78,-23.56,-7.58)	...
14255593+1412101	M0.0	0.150	-3.89	31.36±0.03	9.94e-05	4.48e-04	(68.11,8.69,143.77)	(-42.49,-49.88,-44.76)	...
17150219-3333398	M0.0	...	-1.99	29.45±0.05	...	...	(25.66,-3.36,1.31)	(-29.97,-13.39,-15.20)	...
23301341-2023271	M3.0	...	-3.60	29.08±0.04	...	1.07e-04	(3.57,4.04,-15.02)	(-15.82,-24.87,-1.75)	...
Carina									
08185942-7239561	M0.0	...	-0.68	29.64±0.10	...	1.77e-04	(20.81,-73.25,-27.20)	(-14.42,-30.25,-6.38)	...
Columba									
04322548-3903153	M3.5	...	-5.20	28.92±0.10	...	1.42e-04	(-11.00,-20.94,-22.01)	(-10.04,-3.91,-7.96)	...
05425587-0718382	M3.0	...	-13.96	29.73±0.09	...	2.86e-04	(-66.33,-41.01,-26.15)	(-26.72,-26.73,-12.38)	...
06511418-4037510	non-M	...	1.49	...	...	6.46e-05	(-454.65,-1268.70,-419.99)	(-48.55,-0.76,7.54)	...
07065772-5353463	M0.0	0.380	-1.36	29.66±0.06	4.46e-05	1.83e-04	(-4.32,-43.79,-15.54)	(-10.75,-20.78,-6.24)	Y
23301341-2023271	M3.0	...	-3.60	29.08±0.04	...	1.07e-04	(3.57,4.04,-15.02)	(-15.82,-24.87,-1.75)	...
Tuc-Hor									
02511150-4753077	K5.0	...	-0.83	31.15±0.08	6.83e-05	6.50e-04	(-25.06,-194.89,-324.57)	(2.01,-2.29,18.89)	...
06434532-6424396	M3.0	...	-5.38	28.77±0.18	1.07e-04	5.11e-04	(1.42,-18.25,-8.57)	(-2.75,-19.14,-7.98)	...

4.3.1. *AB Doradus*

In total, we confirm AB Dor membership for 13 previously suggested candidates, and find that 5 previously suggested candidates are not members, as summarized in Table 6. Figure 5 shows the 3D XYZUVW distributions of bona fide members from Gagné et al. (2018a) and newly confirmed members. Figure 6 shows a CMD of previously known members and newly confirmed AB Dor members using *Gaia* DR2 parallaxes and G and  $G_{\text{RP}}$  photometry compared to a volume limited (25 pc) sample of nearby objects. Note that for this CMD (and all CMDs that follow), we plot G- $G_{\text{RP}}$  colors ranging from 0.5 to 2.0 mag to focus on low-mass members of the group. Thus the number of known members plotted in the XYZUVW figure may not match the number of known members plotted in the CMD.

2MASS 01484087–4830519 was posited as a possible Horologium member in Torres et al. (2000). Malo et al. (2013) considered this object to have ambiguous membership, which was revised to possible membership in AB Dor in Malo et al. (2014). 2MASS 05531299–4505119 was found to be a young star in Torres et al. (2006), and was suggested to be an AB Dor candidate in Malo et al. (2014). 2MASS 12383713–2703348 was suggested to be a potential AB Dor member in Malo et al. (2013, 2014), though without a parallax. Binks, & Jeffries (2016) also find 2MASS 12383713–2703348 to be a very likely AB Dor member, again without a parallax. Malo et al. (2013) classified 2MASS 21464282–8543046 as an ambiguous  $\beta$  Pic/Columba/AB Dor candidate, which was then reclassified to an AB Dor candidate in Malo et al. (2014). 2MASS 23115362–4508004 was first found to be a young star in Torres et al. (2006) and was presented as a potential AB Dor member in Torres et al. (2008) and da Silva et al. (2009), though lacking a parallax measurement. Our measured radial velocities, which are consistent with previous measurements, and *Gaia* DR2 parallaxes confirm AB Dor kinematics for all of these objects. Note that 2MASS 01484087–4830519 and 2MASS 23115362–4508004 have co-moving companions in Section 4.2.

2MASS 02130073+1803460 was suggested as a possible AB Dor member in Gagné & Faherty (2018) using *Gaia* DR2 kinematics, but lacking a radial velocity measurement. 2MASS 14415908–1653133 was listed as a weak AB Dor candidate in Gagné et al. (2015a) without a parallax or radial velocity, and is included in Gagné & Faherty (2018) as an AB Dor candidate using its *Gaia* DR2 parallax. 2MASS 04353618–2527347 was suggested to be a possible AB Dor member in Malo et al. (2013) without a radial velocity or parallax measurement. Bartlett et al. (2017) also suggest AB

Dor membership using their parallax measurement of  $57.64 \pm 1.78$  mas, though without a radial velocity measurement. Our measured radial velocities and age diagnostics for these objects confirm AB Dor membership. A co-moving companion to 2MASS 14415908–1653133 was also found in Section 4.2.

2MASS 03100305–2341308 was suggested as a modest probability AB Dor candidate in Riedel et al. (2017) using a radial velocity measurement of  $25.50 \pm 6.12$  km s<sup>-1</sup>, but lacking a distance measurement. Gagné & Faherty (2018) consider this object an AB Dor candidate using kinematic information from *Gaia* DR2. Using our more precise radial velocity ( $24.6 \pm 0.34$  km s<sup>-1</sup>), we confirm the AB Dor kinematics of this star. All youth information is consistent with AB Dor membership, and we consider this a bona fide AB Dor member.

2MASS 04084031–2705473 and 2MASS 04514615–2400087 were considered AB Dor candidates in Malo et al. (2013). Our radial velocity measurements, combined with *Gaia* DR2 parallaxes, show kinematics consistent with AB Dor membership. Age diagnostics agree with AB Dor membership, so we consider both of these objects bona fide members of AB Dor.

2MASS 06373215–2823125 was presented as an AB Dor candidate member in Malo et al. (2013), though the radial velocity measurement in Malo et al. (2014) led the authors to reject AB Dor membership. Our measured radial velocity ( $30.55 \pm 0.64$  km s<sup>-1</sup>) disagrees with the measurement from Malo et al. (2014) ( $17.3 \pm 0.2$  km s<sup>-1</sup>). We find, however, that when our radial velocity is employed, 2MASS 06373215–2823125 shows remarkable agreement with known AB Dor members. We deem 2MASS 06373215–2823125 a bona fide AB Dor member, though a confirming radial velocity measurement is likely warranted.

Malo et al. (2013, 2014) classified 2MASS 21471964–4803166 as an AB Dor candidate without a parallax measurement. Our radial velocity combined with the parallax from *Gaia* DR2 confirms AB Dor membership. Note that BANYAN  $\Sigma$  returns a relatively small probability of AB Dor membership for 2MASS 21471964–4803166 (16.5%). This is due to a slight distance discrepancy, as the optimal predicted distance from BANYAN  $\Sigma$  is  $58.1 \pm 1.8$  pc when the *Gaia* DR2 parallax is not included in the calculation. The actual distance from *Gaia* DR2 is  $63.4 \pm 0.5$  pc, a difference of  $\sim 2.3\sigma$ . Note also that 2MASS 21471964–4803166 has a co-moving companion found in Section 4.2.

2MASS 02523096–1548357, 2MASS 02545247–0709255, 2MASS 04424932–1452268, 2MASS 05130132–7027418, and 2MASS 07115917–3510157 were considered an AB Dor candidates in Malo et al. (2013), while 2MASS



05240991–4223054 was suggested as a AB Dor candidate member in Malo et al. (2013, 2014) without a parallax measurement. Our radial velocity measurements, combined with *Gaia* DR2 parallaxes, rule out AB Dor membership. Note, however, that we consider 2MASS 04424932–1452268 and 2MASS 05240991–4223054 possible fringe AB Dor members in Section 4.4.

#### 4.3.2. *Argus*

Through our kinematic and age analysis, we have confirmed the membership of 7 Argus candidates. We have also rejected 21 previously suggested candidate members. Note that the Argus association has recently been redefined (Zuckerman 2019), which is the likely reason for so many rejected candidates. Many of these rejected candidates are still young based on their age information. Figure 7 shows the 3D XYZUVW distributions of previously known Argus members from Gagné et al. (2018a) and newly confirmed members. We note here that while the newly defined Argus association in Zuckerman (2019) occupies a well-defined area of UVW space, the XYZ distribution of this group is more dispersed than that of most other groups. This may support the assertion that Argus is an unbound association, possibly connected to the open cluster IC 2391 (De Silva et al. 2013). Figure 8 shows a color-magnitude diagram of previously known members and newly confirmed Argus members using *Gaia* DR2 parallaxes and photometry.

2MASS 05471788–2856130 and 2MASS 17275761–4016243 were put forth as ambiguous members of either  $\beta$  Pic or Argus in Malo et al. (2013), without a parallax or radial velocity measurements. 2MASS 12233860–4606203 and 2MASS 22274882–0113527 were originally suggested as Argus candidates in Malo et al. (2013) without radial velocities or parallaxes. Our measured radial velocities along with the parallaxes from *Gaia* DR2, and the age information for these objects confirms Argus membership. Note that 2MASS 17275761–4016243 has a co-moving companion in Section 4.2.

2MASS 09445422–1220544 was a candidate Horologium Association member in Torres et al. (2000). Malo et al. (2013, 2014) suggested Argus membership for this object, but lacked a parallax measurement. Bartlett et al. (2017) reject 2MASS 09445422–1220544 as an Argus member using their parallax, but do not associate it with any other group. Our analysis using our radial velocity and the parallax from *Gaia* DR2 instead confirms 2MASS 09445422–1220544 as an Argus member.

2MASS 10252563–4918389 was suggested as an Argus candidate in Malo et al. (2013, 2014), but lacked a parallax measurement. 2MASS 20072376–5147272 was first

considered an Argus candidate in Torres et al. (2008). It was further considered an Argus candidate in da Silva et al. (2009) and Malo et al. (2013), though lacked a parallax. We confirm 2MASS 10252563–4918389 and 2MASS 20072376–5147272 as Argus members using their *Gaia* DR2 parallaxes and age information from Table 2. Note that a co-moving companion to 2MASS 10252563–4918389 was found in Section 4.2.

Riedel et al. (2014) classified 2MASS 20284361–1128307 as a potential Argus member using their measured parallax, but without a radial velocity. Bowler et al. (2015) also considered 2MASS 20284361–1128307 an Argus candidate (referencing Shkonik et al. in prep). We find that instead that the kinematics and age information for 2MASS 20284361–1128307 better match Carina-Near than Argus.

2MASS 03282609–0537361, 2MASS 03415581–5542287, 2MASS 03415608–5542408, 2MASS 04595855–0333123, 2MASS 06380031–4056011, 2MASS 07343426–2401353, 2MASS 11200609–1029468, 2MASS 13283294–3654233, 2MASS 13382562–2516466, 2MASS 13591045–1950034, 2MASS 19432464–3722108, 2MASS 19435432–0546363, 2MASS 20163382–0711456, and 2MASS 23332198–1240072 were suggested as Argus candidates in Malo et al. (2013) without radial velocity or parallax measurements. 2MASS 00503319+2449009AB, 2MASS 04464970–6034109, and 2MASS 09423823–6229028 were suggested as Argus candidates in Malo et al. (2013, 2014) without parallax measurements. 2MASS 09455843–3253299 was suggested as an Argus candidate in Gagné et al. (2015a) without a parallax or radial velocity measurement. For all of these objects, we find kinematics inconsistent with the Argus association using our measured radial velocities and *Gaia* DR2 parallaxes.

#### 4.3.3. $\beta$ Pictoris

We find 2 new  $\beta$  Pic members, confirm  $\beta$  Pic membership for 7 previously suggested candidates, and reject  $\beta$  Pic membership for 7 previously suggested candidates, as summarized in Table 6. Figure 9 shows the 3D XYZUVW distributions of previously known members from Gagné et al. (2018a) and newly confirmed members. Figure 10 shows a color-magnitude diagram of previously known members and newly confirmed  $\beta$  Pic members using *Gaia* DR2 parallaxes and photometry.

2MASS 02490228–1029220 was suggested as a  $\beta$  Pic member in Bowler et al. (2019). While BANYAN  $\Sigma$  gives a small probability of  $\beta$  Pic membership for this object (2.2%), note that there is no kinematic information for this object from *Gaia* DR2. The photometric distance to this object from Janson et al. (2012) ( $39.0 \pm 7.8$  pc) is consistent with  $\beta$  pic membership ( $57.9 \pm 3.9$ ) con-

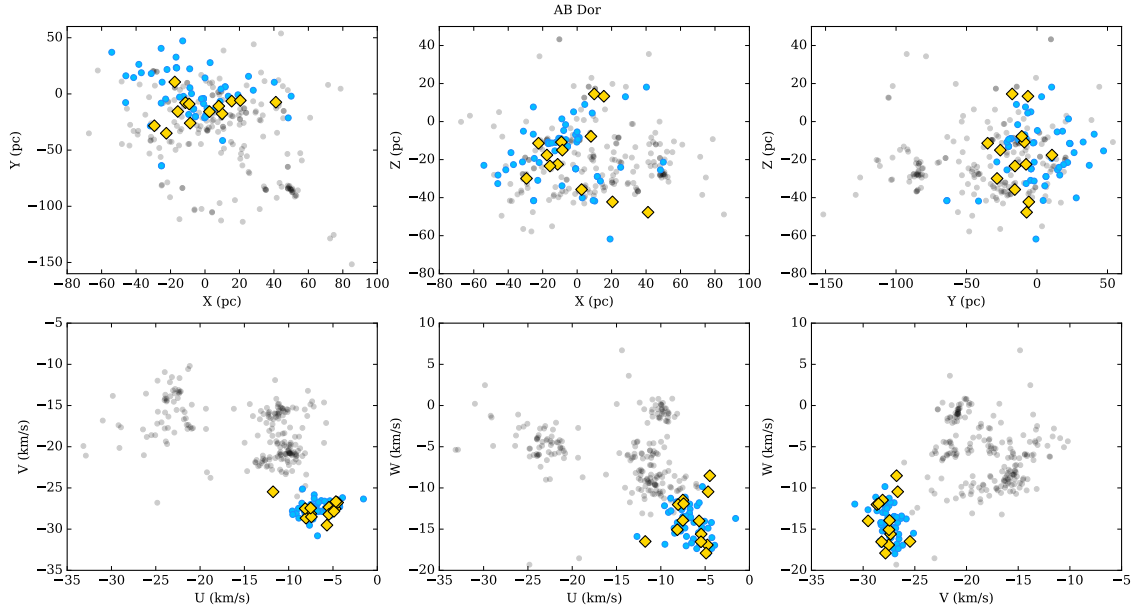


**Figure 5.** A comparison of XYZUVW distributions of previously known AB Dor members from Gagné et al. (2018a) (blue circles) with newly confirmed members (yellow diamonds). Black symbols are bonafide moving group and association members from AB Dor, Argus,  $\beta$  Pic, Carina, Carina-Near, Columba,  $\epsilon$  Cha,  $\eta$  Cha, and Tuc-Hor from Gagné et al. (2018a) for reference.

sidering the large uncertainties inherent in photometric distances, especially for young objects. This star is definitely young considering its clear lithium detection, consistent with  $\beta$  Pic membership. We therefore consider this object a highly likely member of  $\beta$  Pic, where a more accurate distance measurement could be used to further confirm its membership. Note also that this is a close triple system (Bergfors et al. 2010), unresolved in *Gaia* DR2.

2MASS 09462782–4457408 is a new  $\beta$  Pic member with a clear lithium detection, ensuring its youth, and kinematics consistent with known  $\beta$  Pic members. Note that BANYAN also finds a small probability of TW Hya membership for this object (2.5%).

2MASS 02442137+1057411 was suggested as a possible  $\beta$  Pic member in Lépine, & Simon (2009), though was assigned ambiguous membership in Malo et al. (2013), with significant probabilities of belonging to  $\beta$  Pic, Tuc-Hor, and Columba. We present the first radial velocity measurement for this object ( $5.60 \pm 1.09$  km s $^{-1}$ ), which gives this objects similar kinematics with bona fide  $\beta$  Pic members, though it returns a small probability of membership from BANYAN  $\Sigma$  (6.7%). Both the measured radial velocity ( $5.6 \pm 1.1$  km s $^{-1}$ ) and distance ( $48.8 \pm 0.3$  pc) are slightly discrepant from the optimum values from BANYAN  $\Sigma$  ( $11.9 \pm 1.2$  km s $^{-1}$  and  $43.0 \pm 2.6$  pc, respectively), corresponding to differences of  $\sim 2.0\sigma$  and  $\sim 2.7\sigma$ . Considering that this object is certainly young, with a well-measured lithium detection,

we consider it a bona fide  $\beta$  Pic member. Note that this object has a co-moving companion in Section 4.2.

2MASS 05082729–2101444 is a candidate  $\beta$  Pic member discussed in Malo et al. (2013, 2014), Binks & Jeffries (2014), Shkolnik et al. (2017), and Messina et al. (2017). Our measured radial velocity ( $24.94 \pm 0.92$  km s $^{-1}$ ) is more precise than and consistent with those previously measured in Malo et al. (2014) ( $23.5 \pm 1.8$  km s $^{-1}$ ) and Binks & Jeffries (2014) ( $22.8 \pm 3.8$  km s $^{-1}$ ). We investigate the kinematics of this object for the first time using a measured parallax, and find good agreement with known  $\beta$  Pic members, although with a low probability from BANYAN  $\Sigma$  (4.4%). The small probability is due to a mismatch between the predicted distance from BANYAN  $\Sigma$  ( $29.6 \pm 5.5$  pc) and the measured distance from *Gaia* DR2 ( $48.6 \pm 0.2$  pc), a difference of  $\sim 3.3\sigma$ . We consider 2MASS 05082729–2101444 a bona fide  $\beta$  Pic member.

Malo et al. (2013) found 2MASS 05294468–3239141 to be an ambiguous moving group member, then revised that determination in Malo et al. (2014) with a radial velocity measurement (but no parallax), and suggested AB Dor membership. 2MASS 05294468–3239141 was later suggested as a possible  $\beta$  Pic member in Riedel et al. (2014) with a parallax but no radial velocity, and was listed as a candidate  $\beta$  Pic member in Shkolnik et al. (2017) and Messina et al. (2017). Our radial velocity and the parallax from *Gaia* DR2 confirms  $\beta$  Pic kinematics. We deem 2MASS 05294468–3239141 a bona fide  $\beta$  Pic member.

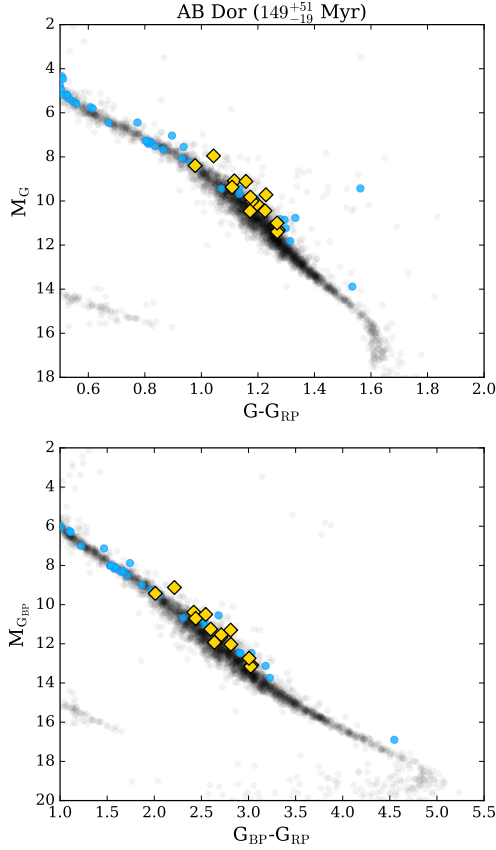


**Figure 6.** CMDs of previously known AB Dor members from Gagné et al. (2018a) (blue circles) with newly confirmed members (yellow diamonds). For reference, we show all objects from *Gaia* DR2 within 25 pc as background gray symbols. The outlier in the upper panel is known AB Dor member Wolf 1225, which likely has an inaccurate *Gaia* G-band magnitude, as this object is not an outlier in the bottom panel which shows  $G_{RP}$  and  $G_{BP}$  magnitudes.

2MASS 05320450–0305291 was presented as a  $\beta$  Pic candidate first in Torres et al. (2008), though lacking radial velocity and parallax measurements. Malo et al. (2013) also suggest  $\beta$  Pic membership without radial velocity or distance information. Elliott et al. (2014) use a radial velocity measurement of  $23.84 \pm 0.55$  km s<sup>-1</sup> and conclude 2MASS 05320450–0305291 is a  $\beta$  Pic member, while Binks, & Jeffries (2016) measure a radial velocity of  $26.2 \pm 1.6$  km s<sup>-1</sup> and reject 2MASS 05320450–0305291 as a potential  $\beta$  Pic member, though neither study had a parallax measurement. 2MASS 16572029–5343316 was listed as a  $\beta$  Pic candidate in Malo et al. (2013) and again in Malo et al. (2014) with a measured radial velocity, but without a parallax.

Malo et al. (2013) listed 2MASS 19233820–4606316 as a potential  $\beta$  Pic member, although without a parallax or radial velocity. Both Moór et al. (2013) and Malo et al. (2014) measured radial velocities for 2MASS 19233820–4606316 consistent with  $\beta$  Pic membership. Using our measured radial velocities and parallaxes from *Gaia* DR2, we find good agreement with known  $\beta$  Pic members for all three objects. We conclude 2MASS 05320450–0305291, 2MASS 16572029–5343316, and 2MASS 19233820–4606316 are bona fide  $\beta$  Pic members. Note that 2MASS 05320450–0305291 has two co-moving companions and 2MASS 16572029–5343316 has a single co-moving companion in Section 4.2.

Malo et al. (2013) first considered 2MASS 13545390–7121476 an AB Dor candidate, then suggested  $\beta$  Pic membership in Malo et al. (2014) after obtaining a radial velocity. Shkolnik et al. (2017) echoes  $\beta$  Pic membership, while Gagné & Faherty (2018) also consider 2MASS 13545390–7121476 a  $\beta$  Pic candidate using its *Gaia* DR2 parallax. We also find strong evidence for  $\beta$  Pic membership, and suggest 2MASS 13545390–7121476 be considered a bona fide  $\beta$  Pic member.

2MASS 05332802–4257205, 2MASS 05422387–2758031, and 2MASS 06135773–2723550 were considered  $\beta$  Pic candidates in Malo et al. (2013), while 2MASS 10571139+0544547 was presented as a  $\beta$  Pic candidate in Schlieder et al. (2012). 2MASS 12115308+1249135 and 2MASS 14255593+1412101 were suggested as a  $\beta$  Pic members in Schlieder et al. (2012). 2MASS 12115308+1249135 was rejected as a possible member in Binks, & Jeffries (2016) based on its radial velocity, while 2MASS 14255593+1412101 was rejected as a possible member in Messina et al. (2017) based on its kinematics. 2MASS 17150219–3333398 was given as a  $\beta$  Pic candidate in Malo et al. (2013, 2014), and is considered a likely  $\beta$  Pic member in Shkolnik et al. (2017), though without a parallax. Our radial velocity measurements, combined with *Gaia* DR2 parallaxes, rule out membership in  $\beta$  Pic.

2MASS 08224744–5726530 was considered an ambiguous candidate in Malo et al. (2013), possibly belonging to  $\beta$  Pic or AB Dor. The radial velocity measurement of this star in Malo et al. (2014) prompted a reclassification to  $\beta$  Pic candidate, which was echoed in Shkolnik et al. (2017). However, using the *Gaia* DR2 parallax for this object, we find that its kinematics do not agree with known  $\beta$  Pic members.

2MASS 23301341–2023271 was initially listed as a  $\beta$  Pic candidate in Malo et al. (2013), while Malo et al. (2014) revised its potential membership status to a Columba candidate based on their radial velocity measurement. Shkolnik et al. (2017) consider 2MASS

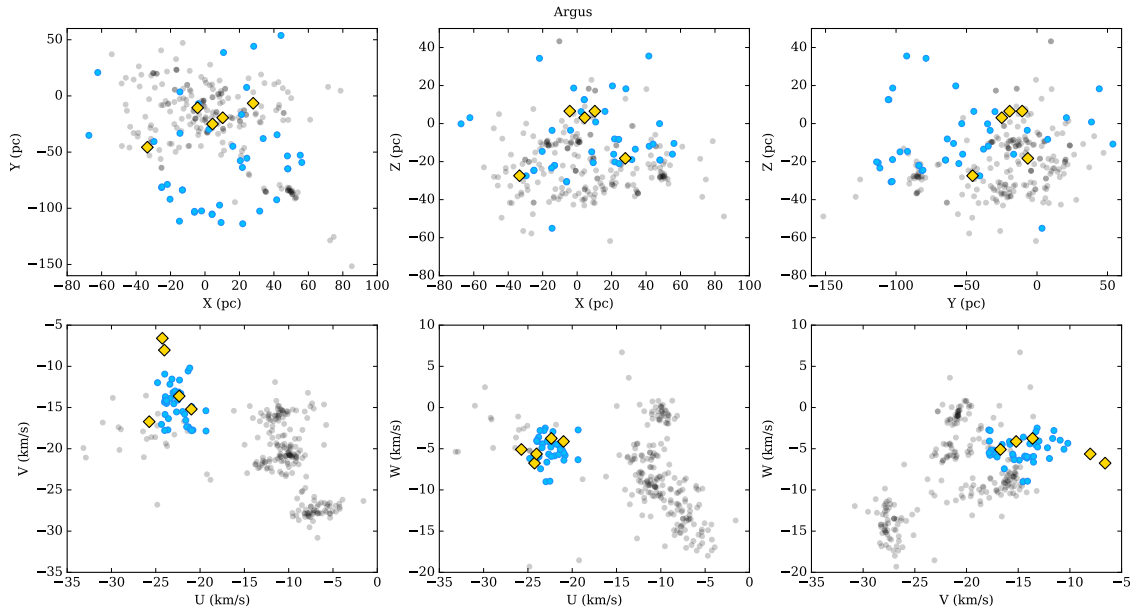


**Figure 7.** A comparison of XYZUVW distributions of previously known Argus members from (blue circles) with newly confirmed members (yellow diamonds), and new discoveries (red squares). Black symbols are the same as in Figure 5.

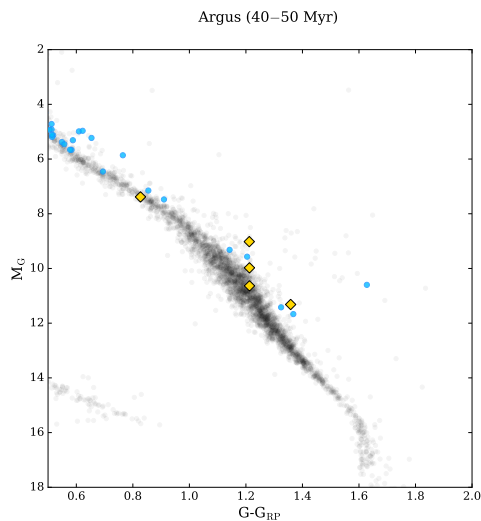


**Figure 8.** CMD of previously known Argus members from Zuckerman (2019) (blue circles) with newly confirmed members (yellow diamonds), and new discoveries (red squares). For reference, we show all objects from *Gaia* DR2 within 25 pc as background gray symbols. The outlier is known Argus member CPD-54 1295, which has poor *Gaia* photometry.

23301341–2023271 a likely member of  $\beta$  Pic. Using our measured radial velocity, which is consistent with the measurement from Malo et al. (2014), and a *Gaia* DR2 parallax, we find that 2MASS 23301341–2023271 does not match well with either group. Note, however that 2MASS 23301341–2023271 is an SB2, and thus likely

warrants a reevaluation once a systemic velocity is measured.

#### 4.3.4. Carina

We find 1 completely new Carina member, reassign membership to Carina for 2 objects previously suggested to belong to different groups, confirm Carina membership for 8 previously suggested candidates, and reject 1 Carina candidate. Figure 11 shows the 3D XYZUVW distributions of previously known members from Gagné et al. (2018a) and newly confirmed Carina members. Figure 12 shows a color-magnitude diagram of previously known and newly confirmed Carina members using *Gaia* DR2 parallaxes and photometry.

2MASS 07065772–5353463 is suggested as a Columba member in Malo et al. (2013, 2014) without a parallax measurement. Using our radial velocity, which is consistent with the value found in Malo et al. (2014), and the *Gaia* DR2 parallax, we find much better agreement with the Carina Association. We consider 2MASS 07065772–5353463 a bona fide Carina member.

2MASS 14284804–7430205 was presented as an Argus candidate in Malo et al. (2013), but was found to not match any groups in Malo et al. (2014) once a radial velocity was measured. Using our more precise radial velocity and the parallax from *Gaia* DR2, we find 2MASS 14284804–7430205 has kinematics consistent with Carina membership. The low probability found using BANYAN  $\Sigma$  for this object (4.2%) is due to discrepant predicted and actual distances ( $62.1 \pm 1.5$  pc and  $58.8 \pm 0.1$  pc, respectively), a difference of  $\sim 2.0\sigma$ .



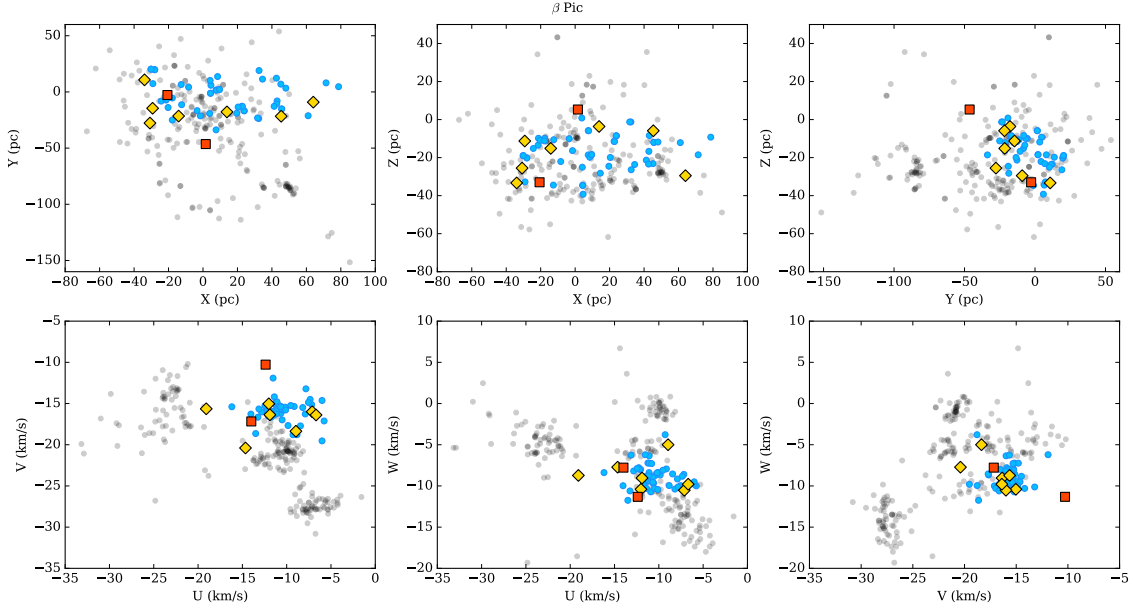


**Figure 9.** A comparison of XYZUVW distributions of previously known  $\beta$  Pic members from (blue circles) with newly confirmed members (yellow diamonds), and new discoveries (red squares). Black symbols are the same as in Figure 5.

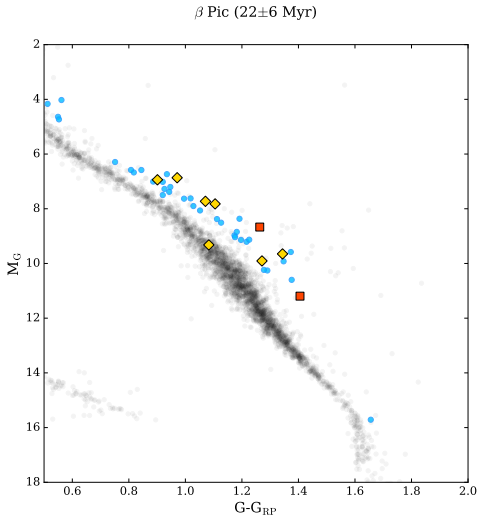


**Figure 10.** CMD of previously known  $\beta$  Pic members from Gagné et al. (2018a) (blue circles) with newly confirmed members (yellow diamonds), and new discoveries (red squares). For reference, we show all objects from *Gaia* DR2 within 25 pc as background gray symbols.

2MASS 06112997–7213388, 2MASS 06234024–7504327, and 2MASS 09032434–6348330 were suggested to be Carina members in Malo et al. (2013, 2014), but without parallax measurements. 2MASS 08412528–5736021 and 2MASS 09315840–6209258 were assigned ambiguous membership in Malo et al. (2013, 2014), with similar probabilities of belonging to Columba or Carina (and  $\beta$  Pic for 2MASS 09315840–6209258). We find good

agreement with known Carina members when using our measured radial velocities and parallaxes from *Gaia* DR2. We consider 2MASS 06112997–7213388, 2MASS 06234024–7504327, 2MASS 09032434–6348330, 2MASS 08412528–5736021, and 2MASS 09315840–6209258 bona fide Carina members. Using our radial velocities and a *Gaia* DR2 parallaxes, we find that these objects match well with known Carina members. All age information is consistent with Carina membership, so we therefore assign 2MASS 08412528–5736021 and 2MASS 09315840–6209258 bona fide Carina membership. 2MASS 08412528–5736021 was also found to have a co-moving companion in Section 4.2.

Gagné & Faherty (2018) suggested 2MASS 08040534–6316396 and 2MASS 09180165–5452332 as possible Carina members using *Gaia* DR2 astrometry, but lacking radial velocities. 2MASS 08040534–6316396 was also suggested as a possible Carina member in Bowler et al. (2019). Our radial velocities, combined with their age information, confirms Carina membership for both objects.

2MASS 08194309–7401232 is presented as a Carina candidate in Gagné et al. (2015b) without a parallax or radial velocity measurement. We confirm this object as a Carina member with our measured radial velocity and the parallax from *Gaia* DR2.

2MASS 08185942–7239561 was considered a Carina candidate in Malo et al. (2013), but was subsequently rejected in Malo et al. (2014), though without a parallax measurement. We agree with this assessment using our radial velocity and the parallax from *Gaia* DR2.

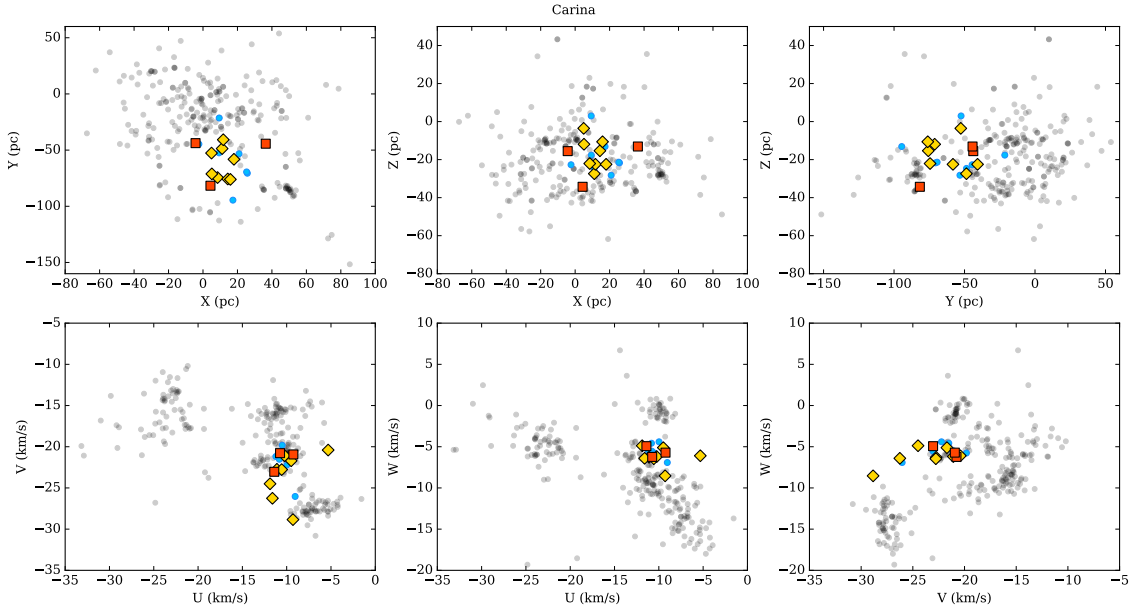


**Figure 11.** A comparison of XYZUVW distributions of previously known Carina members from Gagné et al. (2018a) (blue circles) with newly confirmed members (yellow diamonds), and new discoveries (red squares). Black symbols are the same as in Figure 5.

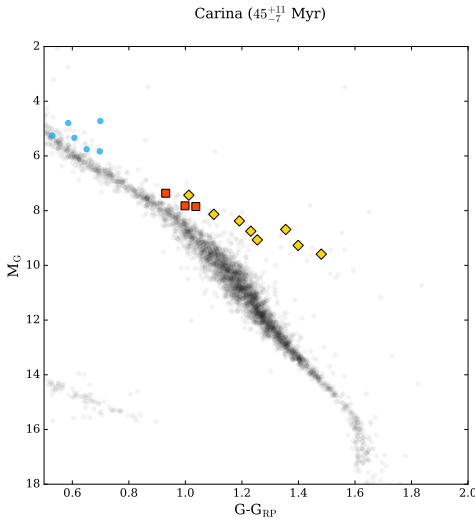


**Figure 12.** CMD of previously known Carina members from Gagné et al. (2018a) (blue circles) with newly confirmed members (yellow diamonds), and new discoveries (red squares). For reference, we show all objects from *Gaia* DR2 within 25 pc as background gray symbols.

#### 4.3.5. Carina-Near

In total, we have discovered one new Carina-Near member, confirming membership for one additional object, and reassigned membership to Carina-Near for 4 objects. Figures 13 and 14 compare the 3D XYZUVW distributions and CMD positions of previously known members from Gagné et al. (2018a)

and newly confirmed Carina-Near members. Interestingly, 2MASS 06134171–2815173 and 2MASS 06380031–4056011 have the latest spectral types of known Carina-Near members (M3.5), with the exception of SIMP J013656.6+093347 (Gagné et al. 2017b).

2MASS 06134171–2815173 is a new Carina-Near member presented in this work. Its kinematics match well with other Carina-Near members, though BANYAN  $\Sigma$  give a relatively low Carina-Near membership probability (9.4%). The small probability is due to a slight mismatch between the predicted distance ( $28.9 \pm 3.8$  pc) and the measured distance ( $41.2 \pm 0.5$  pc), a difference of  $\sim 2.9\sigma$ . However, all youth diagnostics are consistent with the age of Carina-Near ( $\sim 200$  Myr), and thus conclude that 2MASS 06134171–2815173 is a new Carina-Near member. Note that this star is part of a quadruple system found in Section 4.2.

2MASS 06380031–4056011 and 2MASS 19435432–0546363 were suggested to be potential Argus members in Malo et al. (2013) without parallax or radial velocity information. Using parallaxes from *Gaia* DR2 and our measured radial velocities, we instead find excellent agreement with Carina-Near. With age information consistent with Carina-Near membership, we conclude that 2MASS 06380031–4056011 and 2MASS 19435432–0546363 are bona fide Carina-Near members. Note that 2MASS 06380031–4056011 was found to have a co-moving companion in Section 4.2.

Riedel et al. (2014) classified 2MASS 20284361–1128307 as a potential Argus member using their measured par-



allax, but without a radial velocity. Bowler et al. (2015) also considered 2MASS 20284361–1128307 an Argus candidate (referencing Shkonik et al. in prep). We find that 2MASS 20284361–1128307 is a better match to Carina-Near, sharing both age and kinematic properties with known members, even though BANYAN  $\Sigma$  does produce a small but not insignificant probability of belonging to Argus (26.4%).

2MASS 07170438–6311123 was presented as an ambiguous member in Malo et al. (2013), possibly belonging to  $\beta$  Pic, Columba, Carina, or AB Dor. Our measured radial velocity combined with a *Gaia* DR2 parallax rule out membership to all of these groups. We do find, however, a small probability of belonging to Carina-Near from BANYAN  $\Sigma$ . This star is very likely young based on its X-ray luminosity and we include it as a new Carina-Near member.

2MASS 08413264–6825403 was listed as a Carina-Near candidate in Gagné et al. (2018c). We confirm Carina-Near membership for this object using our measured radial velocity and age information.

2MASS 11462310–5238519 was suggested to be a possible Sco-Cen member in Rodriguez et al. (2011) without a parallax or radial velocity. With parallax measurement from *Gaia* DR2 giving a distance within  $\sim 60$  pc, Sco-Cen membership is unlikely. We instead find that 2MASS 11462310–5238519 is a better match to the Carina-Near Association, consistent with the lithium non-detection in its spectrum. We consider 2MASS 11462310–5238519 a new Carina-Near member. Note that this object also has a significant probability of belonging to the Argus association from BANYAN  $\Sigma$  (39.2%), but is a better match to Carina-Near (45.9%).

#### 4.3.6. Columba

In total, we find one new Columba member, confirm 10 previously suggested Columba candidates as new bona fide members, while 5 previously suggested candidates are not found to be non-members. Figure 15 shows the 3D XYZUVW distributions of bona fide members from Gagné et al. (2018a) and newly confirmed members. Figure 16 shows a color-magnitude diagram of previously known members and newly confirmed Columba members using *Gaia* DR2 parallaxes and photometry.

2MASS 03241504–5901125 was suggested to be a possible Horologium Association member in Torres et al. (2000), but was subsequently rejected as a Tuc-Hor member in Zuckerman et al. (2001b). This star was later proposed to be a Columba candidate in Malo et al. (2013, 2014), but lacked a parallax measurement. Our measured radial velocity and the *Gaia* DR2 parallax show that the kinematics of this star are consistent

with the Columba Association, though with a low probability from BANYAN  $\Sigma$  (8.2%). The measured distance ( $86.6 \pm 1.2$  pc) is  $1.1\sigma$  away from the optimum BANYAN  $\Sigma$  distance ( $81.8 \pm 3.2$  pc), while the measured radial velocity ( $18.3 \pm 1.2$  km s $^{-1}$ ) is less than  $1\sigma$  away from the optimum radial velocity ( $16.6 \pm 0.6$  km s $^{-1}$ ). All age diagnostics confirm a young age for this object, and we posit that Columba membership is highly likely.

Malo et al. (2013) proposed 2MASS 03320347–5139550 and 2MASS 05195695–1124440 as possible Columba members, albeit without measured radial velocities or parallaxes. The *Gaia* DR2 parallaxes for these objects, combined with our measured radial velocities confirm Columba kinematics. We consider 2MASS 03320347–5139550 and 2MASS 05195695–1124440 bona fide Columba members, as age indicators for both objects are all consistent with Columba membership. Note that 2MASS 03320347–5139550 and 2MASS 05195695–1124440 both have co-moving companions in Section 4.2.

2MASS 04091413–4008019, 2MASS 05100427–2340407, 2MASS 05100488–2340148, 2MASS 05241317–2104427, 2MASS 05395494–1307598, and 2MASS 05432676–3025129 were proposed as a possible Columba members in Malo et al. (2013, 2014), though without parallax measurements. Our measured radial velocities are consistent with those found in Malo et al. (2014). Combined with the parallax measurements of these objects from *Gaia* DR2, we find space motions consistent with Columba membership, though 2MASS 05432676–3025129 returns a small Columba membership probability from BANYAN  $\Sigma$  (1.3%). This small probability is because the predicted radial velocity ( $22.7 \pm 1.2$  km s $^{-1}$ ) is slightly off from our measured radial velocity ( $28.2 \pm 1.4$  km s $^{-1}$ ), a difference of  $2.1\sigma$ . Because all age information is also consistent with Columba membership, 2MASS 04091413–4008019, 2MASS 05100427–2340407, 2MASS 05100488–2340148, 2MASS 05241317–2104427, 2MASS 05395494–1307598, and 2MASS 05432676–3025129 are deemed to be bona fide Columba members.

Malo et al. (2013, 2014) considered 2MASS 05425587–0718382 a Columba candidate, though without a parallax measurement. While our radial velocity ( $38.81 \pm 5.58$  km s $^{-1}$ ) is less precise than the one presented in Malo et al. (2014) ( $29.7 \pm 3.9$  km s $^{-1}$ ), we find that neither provides a good match to other Columba members when combined with the parallax from *Gaia* DR2. We therefore reject this object as a potential Columba member.

2MASS 06262932–0739540 was deemed an ambiguous Columba candidate in Malo et al. (2013), though lacked radial velocity and parallax measurements. We

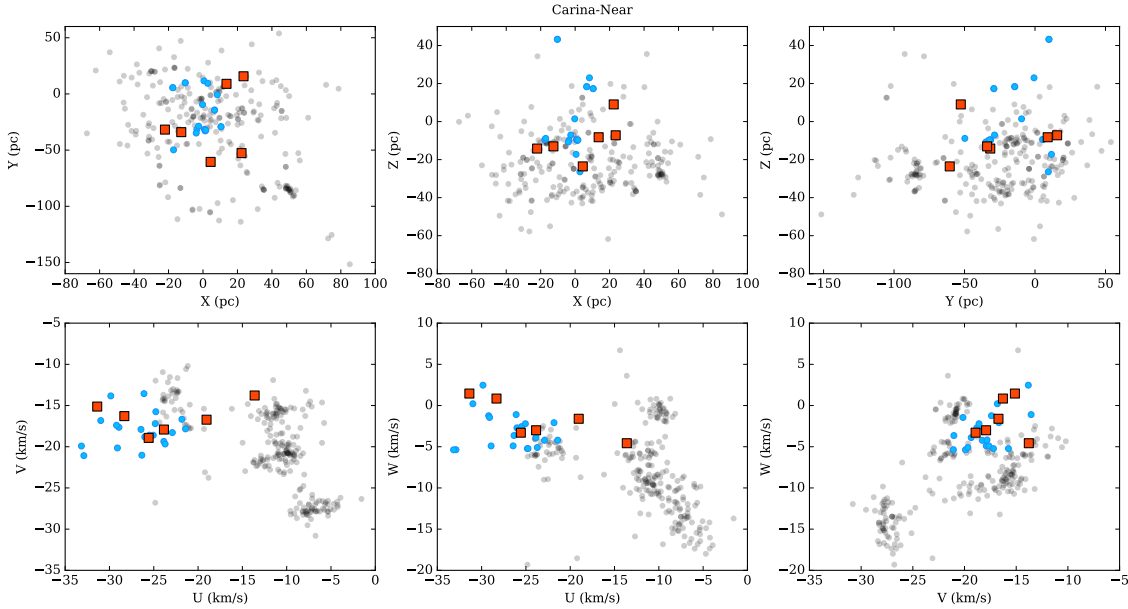


**Figure 13.** A comparison of XYZUVW distributions of previously known Carina-Near members from [Gagné et al. \(2018a\)](#) (blue circles) with newly confirmed members (yellow diamonds), and new discoveries (red squares). Black symbols are the same as in Figure 5.

find good agreement with other Columba members using our measured radial velocity and the parallax from *Gaia* DR2. The well detected lithium for this object confirms its youth, and is consistent with Columba membership. We consider 2MASS 06262932–0739540 a bona fide Columba member.

2MASS 04322548–3903153 was suggested as a Columba candidate member in both [Malo et al. \(2013\)](#) and [Rodríguez et al. \(2013\)](#), though neither study had a radial velocity or parallax for this object. The *Gaia* DR2 parallax, combined with our radial velocity measurement, firmly rule out Columba membership.

[Malo et al. \(2013\)](#) presented 2MASS 06511418–4037510 as a possible Columba member. Our radial velocity measurement, combined with its *Gaia* DR2 parallax, rules out Columba membership. 2MASS 06511418–4037510 is likely a K-type giant based on its small parallax ( $0.7084 \pm 0.0234$  mas).

#### 4.3.7. $\epsilon$ Cha

We confirm the membership of 4  $\epsilon$  Cha members using our measured radial velocities and parallaxes from *Gaia* DR2. Figures 17 and 18 compare the 3D XYZUVW distributions and CMD positions of previously known members from [Gagné et al. \(2018a\)](#) and newly confirmed  $\epsilon$  Cha members.

2MASS 11493184–7851011 was proposed as an  $\epsilon$  Cha member in [Torres et al. \(2008\)](#). It was later proposed to be a potential  $\beta$  Pic member in [Malo et al. \(2013\)](#), though the authors noted that they did not in-

clude  $\epsilon$  Cha as a potential group and a parallax would clear up membership. [Shkolnik et al. \(2017\)](#) determine that 2MASS 11493184–7851011 is a bona fide  $\beta$  Pic member. [Žerjal et al. \(2019\)](#) also suggest 2MASS 11493184–7851011 as an  $\epsilon$  Cha member. We find excellent agreement with  $\epsilon$  Cha and consider this object to be a bona fide  $\epsilon$  Cha member.

2MASS 12194369–7403572 and 2MASS 12202177–7407393 were proposed to be  $\epsilon$  Cha field members in [Torres et al. \(2008\)](#). [Murphy et al. \(2013\)](#) used radial velocity measurements to reinforce membership. Our measured radial velocities and *Gaia* DR2 parallaxes confirm  $\epsilon$  Cha membership. Note that the *Gaia* DR2 parallax uncertainty for 2MASS 12202177–7407393 is atypically large (0.6978 mas), and the reason for the relatively low probability from BANYAN  $\Sigma$  is the discrepancy between its predicted distance ( $99.8 \pm 3.7$  pc) and the measured distance ( $148.9 \pm 15.5$  pc), a difference of  $2.6\sigma$ .

2MASS 12210499–7116493 was suggested as an  $\epsilon$  Cha member in [Kiss et al. \(2011\)](#) with a RAVE radial velocity, but lacking a parallax. Our more precise radial velocity, a parallax from *Gaia* DR2, and a strong lithium detection, confirm  $\epsilon$  Cha membership.

#### 4.3.8. $\eta$ Cha

Our measured radial velocities and the parallaxes from *Gaia* DR2 allow us to confirm the membership of 8  $\eta$  Cha members. Figures 19 and 20 compare the 3D XYZUVW distributions and CMD positions of previously known

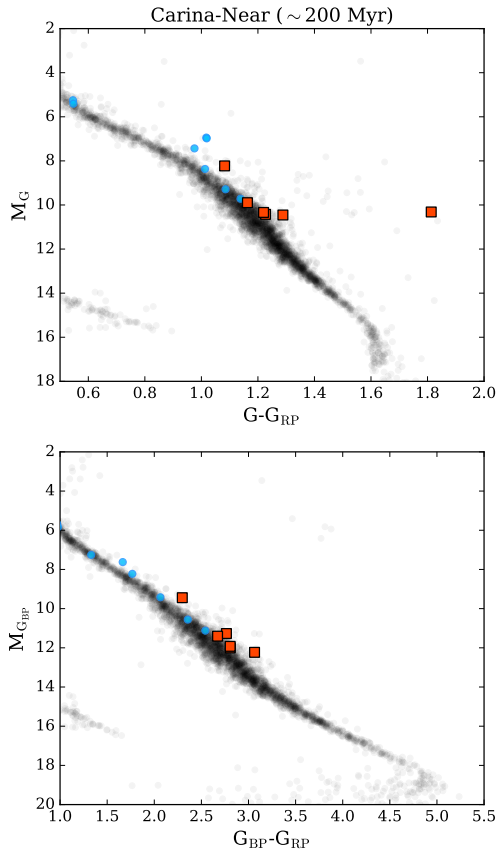


**Figure 14.** CMDs of previously known Carina-Near members from Gagné et al. (2018a) (blue circles) with newly confirmed members (yellow diamonds), and new discoveries (red squares). For reference, we show all objects from *Gaia* DR2 within 25 pc as background gray symbols. The outlying object in the upper panel is 2MASS 06134171–2815173, which likely has an inaccurate *Gaia*, as this object is not an outlier in the bottom panel using *Gaia*  $G_{RP}$  and  $G_{BP}$  magnitudes.

members from Gagné et al. (2018a) and newly confirmed  $\eta$  Cha members.

2MASS 08361072–7908183 and 2MASS 08385150–7916136 were suggested as a members of  $\eta$  Cha in Song et al. (2004) and Lyo et al. (2004). Our radial velocity measurements, plus the *Gaia* DR2 parallaxes confirm  $\eta$  Cha membership.

2MASS 08413030–7853064 was suggested as an  $\eta$  Cha member in Lawson et al. (2002). No radial velocity for this object has been presented previously, and our measurement confirms  $\eta$  Cha membership.

2MASS 08413703–7903304, 2MASS 08422710–7857479, 2MASS 08423879–7854427, and 2MASS 08441637–7859080 were among the original  $\eta$  Cha members proposed in

Mamajek et al. (1999). Remarkably, we find no measurements of their radial velocities anywhere in the literature. We provide the first radial velocities for these objects, all confirming  $\eta$  Cha membership. Note that 2MASS 08441637–7859080 currently lacks astrometry from *Gaia*. The BANYAN  $\Sigma$  percentage in Table 6 uses the statistical distance to this object from Bell et al. (2015) and the proper motion from Zacharias et al. (2017).

2MASS 08440914–7833457 was suggested as an  $\eta$  Cha member in Song et al. (2004). We confirm  $\eta$  Cha membership with our measured radial velocity and the parallax from *Gaia* DR2.

#### 4.3.9. Octans

2MASS 02411909–5725185 was suggested as a possible Octans member using *Gaia* DR2 kinematics (including a radial velocity measurement of  $4.38 \pm 1.77$  km s<sup>-1</sup>) in Gagné & Faherty (2018). Our more precise radial velocity ( $7.03 \pm 0.43$  km s<sup>-1</sup>) returns a 100% probability of matching kinematics to known Octans members using BANYAN  $\Sigma$ . All age information agrees with Octans membership. Note that this star has a co-moving companion in Section 4.2. We do not plot Octans figures, as we have only one confirmed member.

#### 4.3.10. Tucana-Horologium

We reassign membership for 3 objects as Tuc-Hor members, confirm Tuc-Hor membership for 4 previously suggested candidates, and find 2 previously suggested candidates to be non-members. Figure 21 shows the 3D XYZUVW distributions of previously known members from Gagné et al. (2018a) and newly confirmed Tuc-Hor members. Figure 22 shows a color-magnitude diagram of previously known and newly confirmed Tuc-Hor members using *Gaia* DR2 parallaxes and photometry.

2MASS 00153670–2946003 (aka GJ 3017) was suggested as a Tuc-Hor candidate in Gagné & Faherty (2018) using its *Gaia* DR2 parallax and a radial velocity of  $0 \pm 5$  km s<sup>-1</sup> from Bardalez Gagliuffi et al. (2014) (this is likely a mistaken reference, with this measurement being from Kunder et al. 2017). Our more precise radial velocity for this object ( $0.61 \pm 1.31$  km s<sup>-1</sup>) is in agreement with the measurement presented in Gagné & Faherty (2018) and puts 2MASS 00153670–2946003 squarely in the XYZUVW space as bona fide Tuc-Hor members. A lithium non-detection is typical for M4 members of Tuc-Hor (Rodríguez et al. 2013, Kraus et al. 2014), and the X-ray, UV, and H $\alpha$  activity levels of 2MASS 00153670–2946003 are all consistent with Tuc-Hor membership. We conclude that 2MASS 00153670–2946003 is a bona fide member of Tuc-Hor.

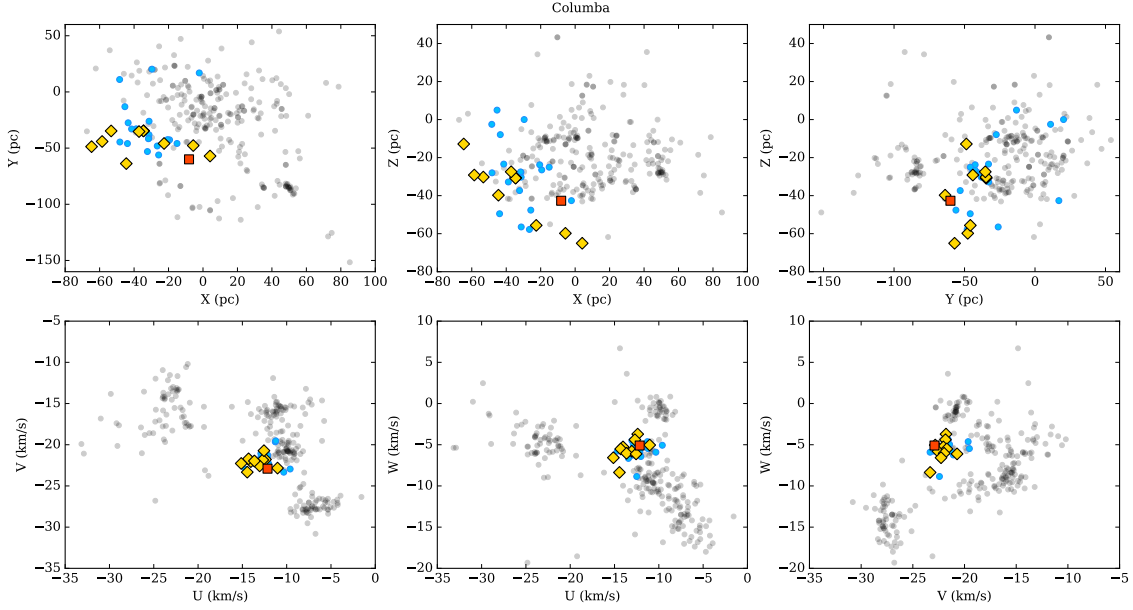


**Figure 15.** A comparison of XYZUVW distributions of previously known Columba members from Gagné et al. (2018a) (blue circles) with newly confirmed members (yellow diamonds), and new discoveries (red squares). Black symbols are the same as in Figure 5.

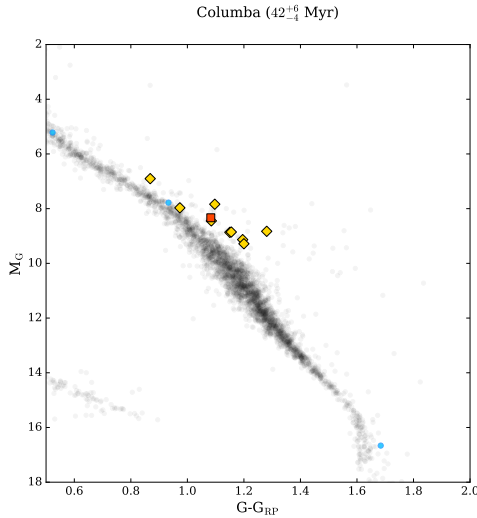


**Figure 16.** CMD of previously known Columba members from Gagné et al. (2018a) (blue circles) with newly confirmed members (yellow diamonds), and new discoveries (red squares). For reference, we show all objects from *Gaia* DR2 within 25 pc as background gray symbols.

2MASS 03454058–7509121, 2MASS 19225071–6310581, and 2MASS 23204705–6723209 were suggested as a Tuc-Hor candidates in Malo et al. (2013, 2014) with a radial velocity measurements of  $13.1 \pm 3.2 \text{ km s}^{-1}$ ,  $6.4 \pm 1.5 \text{ km s}^{-1}$ , and  $6.6 \pm 0.3 \text{ km s}^{-1}$  respectively. Our more precise radial velocities for 2MASS 03454058–7509121 and 2MASS 19225071–6310581 ( $13.81 \pm 0.65 \text{ km s}^{-1}$  and  $0.84 \pm 1.00 \text{ km s}^{-1}$ , respectively) and parallaxes from

*Gaia* DR2 confirm their status as a Tuc-Hor members. Our radial velocity for 2MASS 23204705–6723209 is less precise, though consistent with that measured in Malo et al. (2014) ( $6.13 \pm 1.26 \text{ km s}^{-1}$ ). The *Gaia* DR2 parallax for 2MASS 23204705–6723209 confirms it as a Tuc-Hor member. We also find a co-moving companion to 2MASS 23204705–6723209 in Section 4.2.

2MASS 05142736–1514514 and 2MASS 05142878–1514546 were both assigned ambiguous Tuc-Hor/Columba membership in Malo et al. (2013), and later suggested as Columba candidates in Malo et al. (2014). 2MASS 06002304–4401217 was suggested as potential Columba member in Malo et al. (2013, 2014). We find that the kinematics of all three of these objects make them likely members of Tuc-Hor, which is reflected in their BANYAN  $\Sigma$  probabilities. We consider all three objects Tuc-Hor members. Note that we identify a third component of the 2MASS 05142736–1514514 and 2MASS 05142878–1514546 system, as well as a co-moving companion to 2MASS 06002304–4401217 in Section 4.2.

2MASS 02511150–4753077 and 2MASS 06434532–6424396 were suggested as a members of the Horologium association in Torres et al. (2000). We find that the kinematics of these objects match none of the groups evaluated here.

#### 4.4. Low-Probability Members

The BANYAN  $\Sigma$  algorithm models each association with multivariate Gaussians in six dimensional XYZUVW space (Gagné et al. 2018a). However, mov-

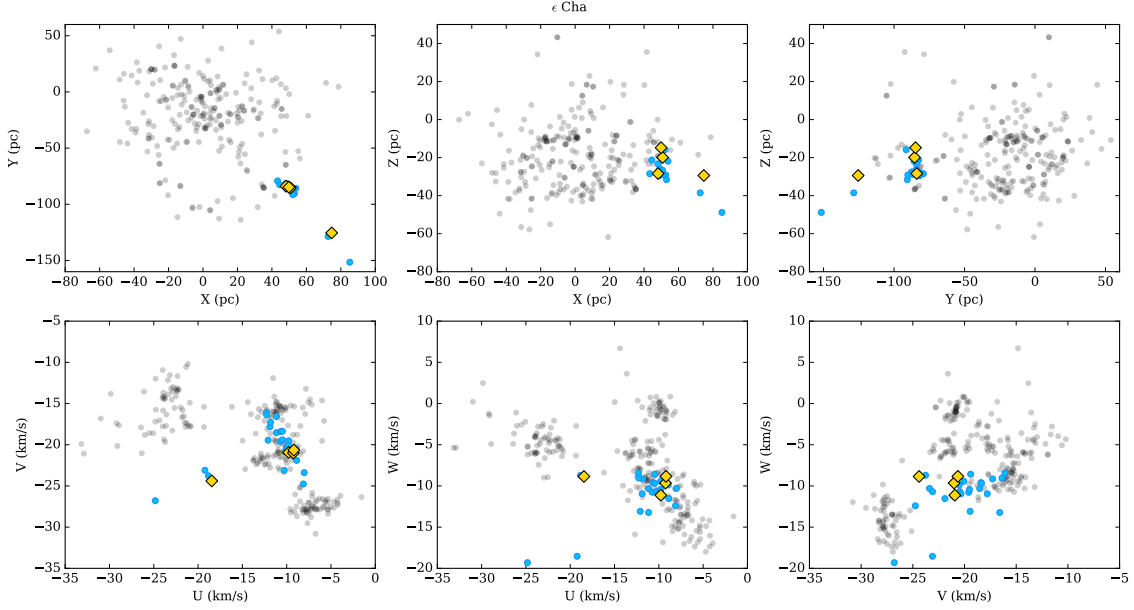


**Figure 17.** A comparison of XYZUVW distributions of previously known  $\epsilon$  Cha members from Gagné et al. (2018a) (blue circles) with newly confirmed members (yellow diamonds). Black symbols are the same as in Figure 5.

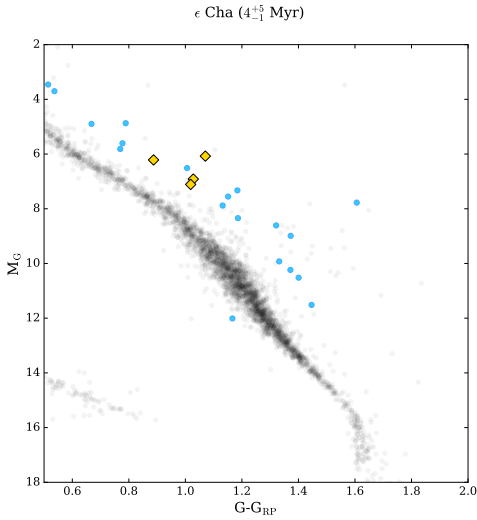


**Figure 18.** CMD of previously known  $\epsilon$  Cha members from Gagné et al. (2018a) (blue circles) with newly confirmed members (yellow diamonds). For reference, we show all objects from *Gaia* DR2 within 25 pc as background gray symbols. The bona fide member below the main-sequence defined by the 25 pc sample is  $\epsilon$  Cha 11, which is thought to be obscured by an circumstellar disk viewed edge-on (Luhman 2004).

ing groups and associations are not necessarily Gaussian in shape (Larson 1981). This also means that groups are constrained by the current census of known members, which in many instances is still incomplete, occasionally leading to low probabilities for high likelihood members (e.g., Lee & Song 2018). For this reason, we performed

an additional check to see if there are any potential group members in our sample missed by the BANYAN framework. We first found the central UVW coordinates of each group considered in Section 4.3 by finding the average position from previously known members from (Gagné et al. 2018a) combined with newly confirmed members from this work. We then calculate the dispersion in U, V, and W and search for objects within  $3\sigma$  of each velocity component. We excluded objects that were previously determined to be a member of a group in Section 4.3 and objects with large astrometric uncertainties (e.g., objects without *Gaia* parallaxes). Seven objects were found to match the kinematics of a known group. We consider these objects possible members, and provide their information in Table 8. We also include the  $\sigma$  difference between the optimal distance and radial velocity values from BANYAN  $\Sigma$  and those measured in this work defined as the difference between the optimal and measured values divided by the combined uncertainty.

2MASS 04424932–1452268 and 2MASS 05240991–4223054 were rejected as AB Dor members in Section 4.3.1, but we find them to be potential fringe members of AB Dor here. All age diagnostics are consistent with AB Dor membership for both objects. 2MASS 07343426–2401353, 2MASS 09423823–6229028, and 2MASS 13591045–1950034 were all rejected as Argus members in Section 4.3.2, however we find that they are potential edge members of Carina-Near. Note that 2MASS 07343426–2401353 is also found to be a possible fringe member of Columba. 2MASS 07343426–2401353



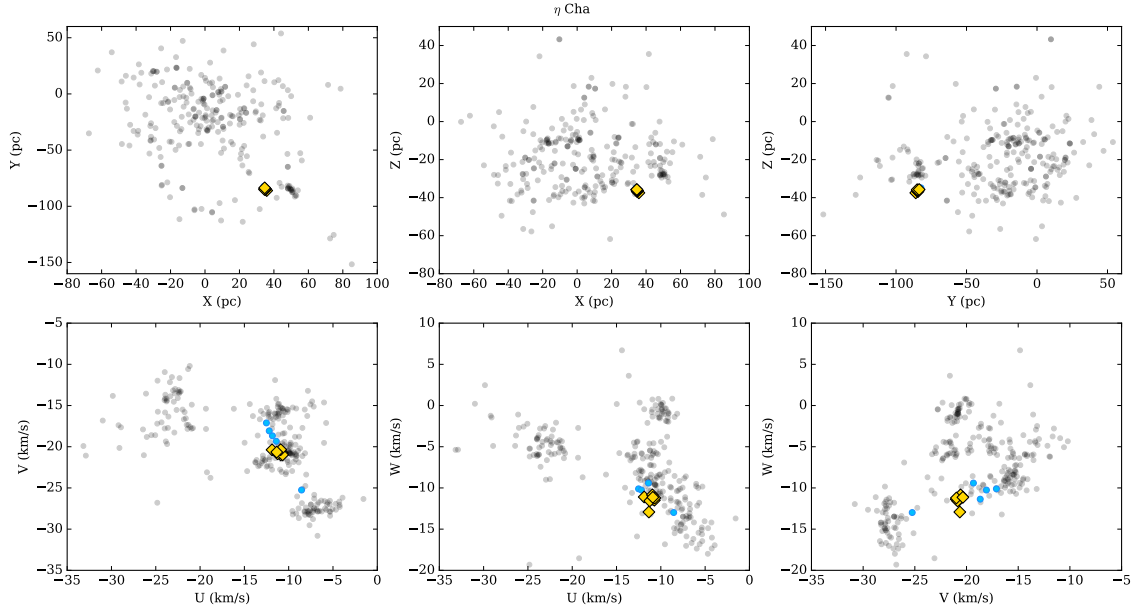


**Figure 19.** A comparison of XYZUVW distributions of previously known  $\eta$  Cha members from Gagné et al. (2018a) (blue circles) with newly confirmed members (yellow diamonds). Black symbols are the same as in Figure 5.

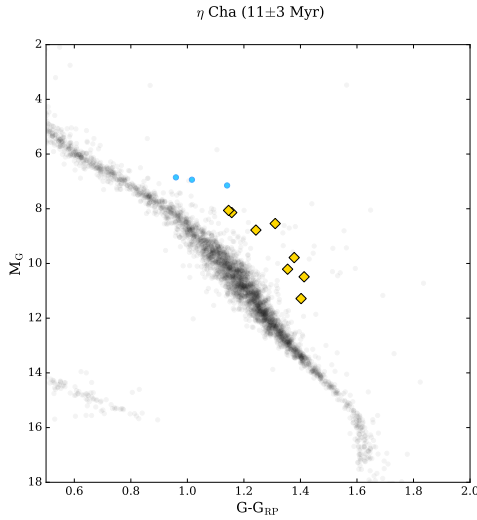


**Figure 20.** CMD of previously known  $\eta$  Cha members from Gagné et al. (2018a) (blue circles) with newly confirmed members (yellow diamonds). For reference, we show all objects from *Gaia* DR2 within 25 pc as background gray symbols.

was rejected as a potential  $\beta$  Pic member in Section 4.3.3, and we find it to be a potential Carina-Near member here. Age diagnostics are consistent with Carina-Near for all four objects. Lastly, 2MASS 11091606–7352465 is found to be a potential member of AB Dor,  $\beta$  Pic, or Carina. This object was also found to have ambiguous moving group membership in Malo et al. (2014), possibly belonging to  $\beta$  Pic, Carina, or Argus. The CMD position and age diagnostics for 2MASS 11091606–7352465 are more consistent with  $\beta$  Pic and Carina than AB Dor.

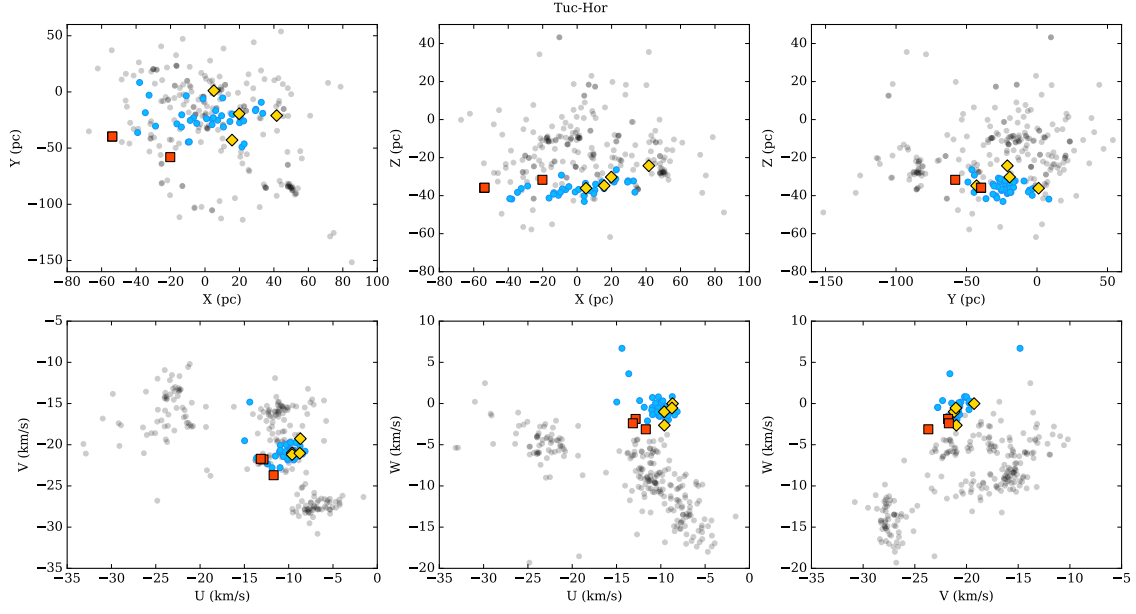


**Figure 21.** A comparison of XYZUVW distributions of previously known Tuc-Hor members from [Gagné et al. \(2018a\)](#) (blue circles) with newly confirmed members (yellow diamonds), and new discoveries (red squares). Black symbols are the same as in Figure 5.

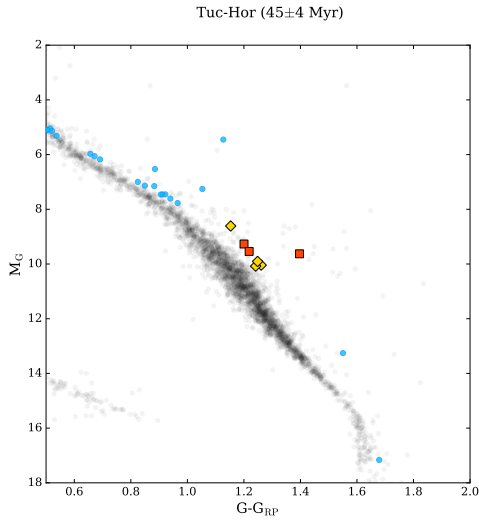


**Figure 22.** CMD of previously known Tuc-Hor members from [Gagné et al. \(2018a\)](#) (blue circles) with newly confirmed members (yellow diamonds), and new discoveries (red squares). For reference, we show all objects from *Gaia* DR2 within 25 pc as background gray symbols.

Table 8. Low-Probability Candidate Members

2MASS	Spec.	Li EW <sup>a</sup>	H $\alpha$ EW	$\log L_X$	$f_{FUV}/f_J$	$f_{NUV}/f_J$	XYZ	UVW	$\sigma_{\text{dist}}$	$\sigma_{\text{RV}}$
Name	Type	( $\text{\AA}$ )	( $\text{\AA}$ )	( $\text{erg s}^{-1}$ )			(pc)	( $\text{km s}^{-1}$ )		
AB Dor										
04424932-1452268	M4.0	...	-6.00	29.00 $\pm$ 0.10	...	1.75e-04	(-24.41,-15.55,-20.33)	(-1.67,-30.52,-13.76)	4.45	0.16
05240991-4223054	M0.5	...	-2.41	29.80 $\pm$ 0.09	...	1.84e-04	(-31.89,-77.48,-55.42)	(-11.00,-31.02,-11.84)	3.08	1.74
11091606-7352465	M3.0	...	-3.49	29.59 $\pm$ 0.13	6.03e-05	2.25e-04	(27.81,-57.30,-14.03)	(-7.11,-24.57,-7.39)	1.80	1.60
$\beta$ Pic										
11091606-7352465	M3.0	...	-3.49	29.59 $\pm$ 0.13	6.03e-05	2.25e-04	(27.81,-57.30,-14.03)	(-7.11,-24.57,-7.39)	1.76	2.48
Carina										
11091606-7352465	M3.0	...	-3.49	29.59 $\pm$ 0.13	6.03e-05	2.25e-04	(27.81,-57.30,-14.03)	(-7.11,-24.57,-7.39)	4.34	1.68
Carina-Near										
07343426-2401353	M3.5	...	-6.19	29.06 $\pm$ 0.13	...	...	(-21.54,-35.95,-1.41)	(-16.88,-18.69,-3.72)	3.15	0.47
08224744-5726530	M4.5	...	-6.09	28.34 $\pm$ 0.05	...	...	(0.56,-12.64,-2.56)	(-36.48,-15.61,-5.83)	8.84	2.99
09423823-6229028	M3.5	...	-1.24	29.19 $\pm$ 0.10	...	...	(9.44,-41.05,-5.31)	(-30.35,-18.15,-8.55)	8.80	2.22
13591045-1950034	M4.5	...	-4.63	28.33 $\pm$ 0.07	1.66e-05	6.18e-05	(6.68,-4.86,6.99)	(-28.11,-16.99,-9.81)	1.07	5.85
Columba										
07343426-2401353	M3.5	...	-6.19	29.06 $\pm$ 0.13	...	...	(-21.54,-35.95,-1.41)	(-16.88,-18.69,-3.72)	5.02	1.53



#### 4.5. The Age of Carina

The Carina association was originally part of a larger complex named GAYA2 in Torres et al. (2001) which included Carina, Tuc-Hor, and Columba, all of which were proposed to have similar ages ( $\sim 30$  Myr; Torres et al. 2001). GAYA2 was eventually divided into Carina, Tuc-Hor, and Columba, with an updated list of Carina members in Torres et al. (2008). The age most often quoted for Carina, which we quote in this work, is  $45_{-7}^{+11}$  from Bell et al. (2015), which is based on isochronal fitting to 12 group members, the lowest number of objects fit for a group in that work. Furthermore, only 5 of the 12 objects examined had measured parallaxes, all with spectral types earlier than K2. The remaining 7 objects (spectral types K7 to M4.5) only had statistical distances from either Malo et al. (2013) or Malo et al. (2014).

We note that the confirmed members of Carina found in this work are elevated above the main sequence more than expected in Figure 12. For an empirical comparison, we plotted the CMD distribution of Carina members versus the presumed similar age Tuc-Hor association members found in Section 4.3.10 and the younger  $\beta$  Pic group association in Figure 23. While there is scatter among all groups, Carina members tend to rest higher above the main sequence than members of Tuc-Hor and more closely follow the sequence defined by  $\beta$  Pic members, suggesting a younger age.

We also compare the lithium abundances of Carina members versus those from  $\beta$  Pic and Tuc-Hor. We took lithium abundances for  $\beta$  Pic members from Shkolnik et al. (2017), and Kraus et al. (2014) for Tuc-Hor. For Carina members, we use the compilation of lithium measurements from Riedel et al. (2017). A comparison of lithium abundances is shown in Figure 24. While there is a dearth of known Carina members with spectral types between K2 and M0, the strong lithium detections for several members with spectral types  $\geq M0$  and  $< M2$  implies a younger age than Tuc-Hor, which is depleted for spectral types K7–M5. The observed lithium abundances are more consistent with  $\beta$  Pic, which is depleted for spectral types M1–M4. Note that Murphy et al. (2018) find an age for the disk-hosting Carina member WISE J0808–6443 (Silverberg et al. 2016) of  $33_{-15}^{+25}$  Myr. If a younger age is indeed warranted for Carina, the protoplanetary disk found around WISE J0808–6443 may pose less of a challenge to disk lifetime models. A more thorough census of Carina membership could help to determine a more precise lithium depletion boundary age.

#### 5. CONCLUSION

Using high-resolution optical spectra, we measured radial velocities and H $\alpha$  and Li  $\lambda 6707$  equivalent widths for 336 candidate low-mass stars, with the aim of identifying new young stars in the solar neighborhood. Combining our radial velocities with astrometry from *Gaia* DR2, we calculated 3D kinematics for each member, and evaluated their potential membership in known moving groups and associations. We discovered 4 completely new moving group members, reassigned membership for 10 objects, and confirmed association membership for 62 additional stars. We further rejected 44 suggested members, highlighting the importance of full kinematics when evaluating moving group membership. We also investigated our measured H $\alpha$  equivalent widths for evidence of ongoing accretion, and find 5 likely accretors within our sample. We used *Gaia* DR2 astrometry to search for co-moving companions to objects in our sample, identifying 69 co-moving systems. In addition, we found that the age diagnostics for previously known and new Carina members confirmed in this work indicate an age nearer to that of  $\beta$  Pic ( $\sim 22$  Myr), half the age of previous estimates. Our catalog also contains numerous additional young stars that do not belong to any currently known moving groups or associations. Such objects may help to locate and define new young groups in the solar neighborhood.

A.S. and E.S. appreciate support from NASA/Habitable Worlds grant NNX16AB62G (PI E. Shkolnik). This work has made use of data from the European Space Agency (ESA) mission *Gaia* (<https://www.cosmos.esa.int/gaia>), processed by the *Gaia* Data Processing and Analysis Consortium (DPAC, <https://www.cosmos.esa.int/web/gaia/dpac/consortium>). Funding for the DPAC has been provided by national institutions, in particular the institutions participating in the *Gaia* Multilateral Agreement. This work is based on observations made with the NASA Galaxy Evolution Explorer. *GALEX* is operated for NASA by the California Institute of Technology under NASA contract NAS5-98034. This publication makes use of data products from the Two Micron All Sky Survey, which is a joint project of the University of Massachusetts and the Infrared Processing and Analysis Center/California Institute of Technology, funded by the National Aeronautics and Space Administration and the National Science Foundation. This research has made use of the SIMBAD database, operated at CDS, Strasbourg, France.

#### REFERENCES

- Andersen, J., Nordstrom, B., Ardeberg, A., et al. 1985, *Astronomy and Astrophysics Supplement Series*, 59, 15
- Bardalez Gagliuffi, D. C., Burgasser, A. J., Gelino, C. R., et al. 2014, *ApJ*, 794, 143

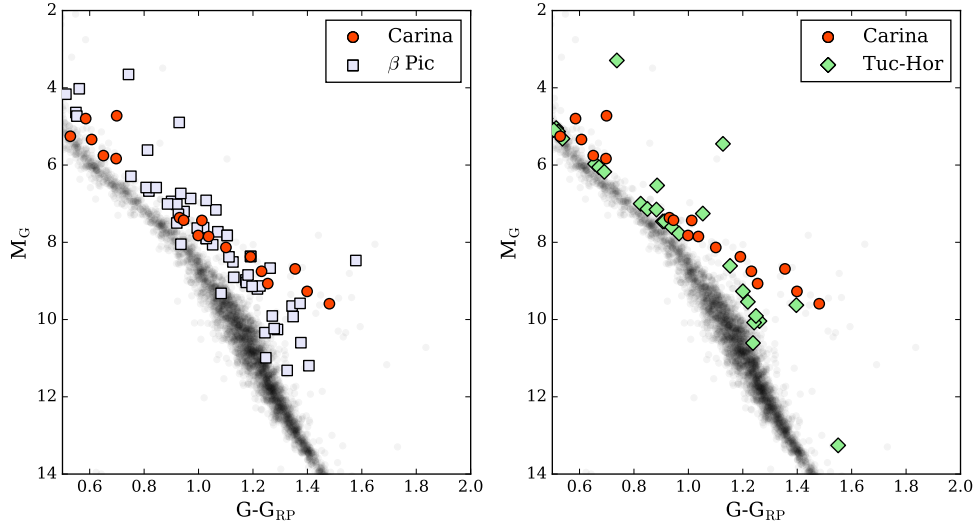


**Figure 23.** CMD of previously known, new, and confirmed Carina members with members of the  $\beta$  Pictoris moving group (left) and members of the Tucana-Horologium association (right). For reference, we show all objects from *Gaia* DR2 within 25 pc as background gray symbols.

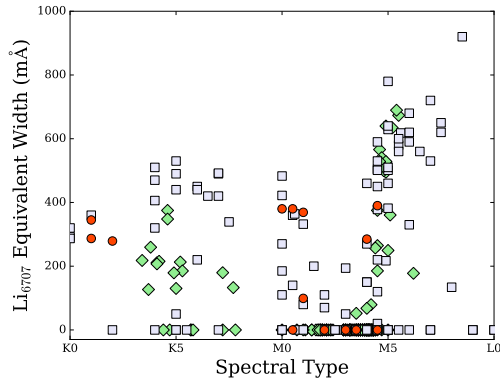


**Figure 24.** Lithium  $\lambda 6707$  abundances of Carina members (red circles) compared to those of the  $\beta$  Pictoris moving group and the Tuc-Hor association.

Barrado y Navascués, D., & Martín, E. L. 2003, *AJ*, 126, 2997  
 Bartlett, J. L., Lurie, J. C., Riedel, A., et al. 2017, *AJ*, 154, 151.  
 Bell, C. P. M., Mamajek, E. E., & Naylor, T. 2015, *MNRAS*, 454, 593  
 Bergfors, C., Brandner, W., Janson, M., et al. 2010, *A&A*, 520, A54.  
 Best, W. M. J., Magnier, E. A., Liu, M. C., et al. 2018, *The Astrophysical Journal Supplement Series*, 234, 1  
 Binks, A. S., & Jeffries, R. D. 2014, *MNRAS*, 438, L11  
 Binks, A. S., Jeffries, R. D., & Maxted, P. F. L. 2015, *MNRAS*, 452, 173  
 Binks, A. S., & Jeffries, R. D. 2016, *MNRAS*, 455, 3345

Binks, A. S., & Jeffries, R. D. 2017, *MNRAS*, 469, 579  
 Blake, C. H., Charbonneau, D., White, R. J., et al. 2007, *ApJ*, 666, 1198  
 Blake, C. H., Charbonneau, D., & White, R. J. 2010, *ApJ*, 723, 684  
 Bochanski, J. J., Hawley, S. L., Reid, I. N., et al. 2005, *AJ*, 130, 1871  
 Bobylev, V. V., Goncharov, G. A., & Bajkova, A. T. 2006, *Astronomy Reports*, 50, 733  
 Boller, T., Freyberg, M. J., Trümper, J., et al. 2016, *A&A*, 588, A103  
 Bowler, B. P., Liu, M. C., Shkolnik, E. L., & Dupuy, T. J. 2013, *ApJ*, 774, 55  
 Bowler, B. P., Shkolnik, E. L., Liu, M. C., et al. 2015, *ApJ*, 806, 62.  
 Bowler, B. P., Liu, M. C., Mawet, D., et al. 2017, *AJ*, 153, 18  
 Bowler, B. P., Hinkley, S., Ziegler, C., et al. 2019, *arXiv:1903.06303*  
 Brewer, J. M., Fischer, D. A., Valenti, J. A., et al. 2016, *The Astrophysical Journal Supplement Series*, 225, 32  
 Burgasser, A. J., Logsdon, S. E., Gagné, J., et al. 2015, *The Astrophysical Journal Supplement Series*, 220, 18  
 Chauvin, G., Lagrange, A.-M., Dumas, C., et al. 2004, *A&A*, 425, L29  
 Chauvin, G., Lagrange, A.-M., Dumas, C., et al. 2005, *A&A*, 438, L25  
 Chauvin, G., Desidera, S., Lagrange, A.-M., et al. 2017, *A&A*, 605, L9

- Chubak, C., Marcy, G., Fischer, D. A., et al. 2012, arXiv:1207.6212
- Cook, N. J., Pinfield, D. J., Marocco, F., et al. 2016, MNRAS, 457, 2192
- Covino, E., Alcalá, J. M., Allain, S., et al. 1997, A&A, 328, 187
- Cruz, K. L., Reid, I. N., Liebert, J., et al. 2003, AJ, 126, 2421
- Cutispoto, G., Tagliaferri, G., Pallavicini, R., et al. 1996, Astronomy and Astrophysics Supplement Series, 115, 41
- da Silva, L., Torres, C. A. O., de La Reza, R., et al. 2009, A&A, 508, 833
- de la Reza, R., & Pinzón, G. 2004, AJ, 128, 1812
- De Silva, G. M., D’Orazi, V., Melo, C., et al. 2013, MNRAS, 431, 1005
- de Zeeuw, P. T., Hoogerwerf, R., de Bruijne, J. H. J., Brown, A. G. A., & Blaauw, A. 1999, AJ, 117, 354
- Delfosse, X., Forveille, T., Perrier, C., et al. 1998, A&A, 331, 581
- Deshpande, R., Martín, E. L., Montgomery, M. M., et al. 2012, AJ, 144, 99
- Desidera, S., Covino, E., Messina, S., et al. 2015, A&A, 573, A126
- Dittmann, J. A., Irwin, J. M., Charbonneau, D., & Berta-Thompson, Z. K. 2014, ApJ, 784, 156
- Donaldson, J. K., Weinberger, A. J., Gagné, J., et al. 2016, ApJ, 833, 95
- Donati, J.-F., Catala, C., Landstreet, J. D., & Petit, P. 2006, Solar Polarization 4, 358, 362
- Donati, J.-F., Jardine, M. M., Gregory, S. G., et al. 2007, MNRAS, 380, 1297
- Dupuy, T. J., & Liu, M. C. 2012, ApJS, 201, 19
- Dupuy, T. J., Liu, M. C., Allers, K. N., et al. 2018, AJ, 156, 57
- Elliott, P., Bayo, A., Melo, C. H. F., et al. 2014, A&A, 568, A26
- Faherty, J. K., Riedel, A. R., Cruz, K. L., et al. 2016, The Astrophysical Journal Supplement Series, 225, 10
- Faherty, J. K., Bochanski, J. J., Gagné, J., et al. 2018, ApJ, 863, 91
- Fernández, D., Figueras, F., & Torra, J. 2008, A&A, 480, 735
- Finch, C. T., Zacharias, N., Subasavage, J. P., Henry, T. J., & Riedel, A. R. 2014, AJ, 148, 119
- Finch, C. T., & Zacharias, N. 2016, AJ, 151, 160
- Finch, C. T., Zacharias, N., & Jao, W.-C. 2018, AJ, 155, 176
- Frasca, A., Guillout, P., Klutsch, A., et al. 2018, A&A, 612, A96
- Gagné, J., Lafrenière, D., Doyon, R., Malo, L., & Artigau, É. 2015a, ApJ, 798, 73
- Gagné, J., Faherty, J. K., Cruz, K. L., et al. 2015b, The Astrophysical Journal Supplement Series, 219, 33
- Gagné, J., Faherty, J. K., Mamajek, E. E., et al. 2017a, The Astrophysical Journal Supplement Series, 228, 18
- Gagné, J., Faherty, J. K., Burgasser, A. J., et al. 2017b, ApJL, 841, L1
- Gagné, J., Mamajek, E. E., Malo, L., et al. 2018a, ApJ, 856, 23
- Gagné, J., & Faherty, J. K. 2018, ApJ, 862, 138
- Gagné, J., Roy-Loubier, O., Faherty, J. K., Doyon, R., & Malo, L. 2018c, ApJ, 860, 43
- Gagné, J., Faherty, J. K., & Mamajek, E. E. 2018d, ApJ, 865, 136
- Gaia Collaboration, Prusti, T., de Bruijne, J. H. J., et al. 2016, A&A, 595, A1
- Gaia Collaboration, Brown, A. G. A., Vallenari, A., et al. 2018, A&A, 616, A1
- Gaidos, E., Mann, A. W., Lépine, S., et al. 2014, MNRAS, 443, 2561
- Gizis, J. E., Reid, I. N., & Hawley, S. L. 2002, AJ, 123, 3356
- Gliese, W., & Jahreiß, H. 1991, On: The Astronomical Data Center CD-ROM: Selected Astronomical Catalogs, Vol. I, ed. L.E. Brodzmann, & S.E. Gesser, (Greenbelt, MD: Goddard Space Flight Center)
- Gontcharov, G. A. 2006, Astronomy Letters, 32, 759
- Gould, A., & Chanamé, J. 2004, ApJS, 150, 455
- Gray, R. O., Corbally, C. J., Garrison, R. F., et al. 2006, AJ, 132, 161
- Guenther, E. W., Esposito, M., Mundt, R., et al. 2007, A&A, 467, 1147
- Guo, Y.-X., Yi, Z.-P., Luo, A.-L., et al. 2015, Research in Astronomy and Astrophysics, 15, 1182
- Hawley, S. L., Gizis, J. E., & Reid, I. N. 1996, AJ, 112, 2799
- Hollands, M. A., Tremblay, P.-E., Gänsicke, B. T., Gentile-Fusillo, N. P., & Toonen, S. 2018, MNRAS, 480, 3942
- Huélamo, N., Vaz, L. P. R., Torres, C. A. O., et al. 2009, A&A, 503, 873
- Janson, M., Hormuth, F., Bergfors, C., et al. 2012, ApJ, 754, 44
- Janson, M., Bergfors, C., Brandner, W., et al. 2014, ApJS, 214, 17
- Jordi, C., Gebran, M., Carrasco, J. M., et al. 2010, A&A, 523, A48.
- Kastner, J. H., Zuckerman, B., Weintraub, D. A., & Forveille, T. 1997, Science, 277, 67
- Kastner, J. H., Sacco, G., Rodriguez, D., et al. 2017, ApJ, 841, 73

- Kelson, D. D., Illingworth, G. D., van Dokkum, P. G., & Franx, M. 2000, *ApJ*, 531, 159
- Kelson, D. D. 2003, *PASP*, 115, 688
- Kharchenko, N. V., Scholz, R.-D., Piskunov, A. E., et al. 2007, *Astronomische Nachrichten*, 328, 889
- Kirkpatrick, J. D., Cruz, K. L., Barman, T. S., et al. 2008, *ApJ*, 689, 1295
- Kiss, L. L., Moór, A., Szalai, T., et al. 2011, *MNRAS*, 411, 117
- Kraus, A. L., Shkolnik, E. L., Allers, K. N., & Liu, M. C. 2014, *AJ*, 147, 146
- Krautter, J., Wichmann, R., Schmitt, J. H. M. M., et al. 1997, *Astronomy and Astrophysics Supplement Series*, 123, 329
- Kunder, A., Kordopatis, G., Steinmetz, M., et al. 2017, *AJ*, 153, 75
- Lagrange, A.-M., Bonnefoy, M., Chauvin, G., et al. 2010, *Science*, 329, 57
- Larson, R. B. 1981, *MNRAS*, 194, 809
- Lawson, W. A., Crause, L. A., Mamajek, E. E., & Feigelson, E. D. 2002, *MNRAS*, 329, L29
- Lee, J., & Song, I. 2018, *MNRAS*, 475, 2955
- Lépine, S., & Simon, M. 2009, *AJ*, 137, 3632
- Lépine, S., & Gaidos, E. 2011, *AJ*, 142, 138
- Liu, M. C., Dupuy, T. J., & Allers, K. N. 2016, *ApJ*, 833, 96
- Lodieu, N., Scholz, R. D., McCaughrean, M. J., et al. 2005, *A&A*, 440, 1061
- Looper, D. L., Bochanski, J. J., Burgasser, A. J., et al. 2010, *AJ*, 140, 1486.
- Looper, D. L. 2011, Ph.D. Thesis,
- Luhman, K. L. 2004, *ApJ*, 616, 1033.
- Luo, A.-L., Zhao, Y.-H., Zhao, G., et al. 2015, *Research in Astronomy and Astrophysics*, 15, 1095
- Luo, A.-L., Zhou, Y.-H., Zhao, G., et al. 2016, *Vizie Online Data Catalog*, 5149
- Lyo, A.-R., Lawson, W. A., Feigelson, E. D., & Crause, L. A. 2004, *MNRAS*, 347, 246
- Macintosh, B., Graham, J. R., Barman, T., et al. 2015, *Science*, 350, 64
- Maldonado, J., Martínez-Arnáiz, R. M., Eiroa, C., et al. 2010, *A&A*, 521, A12
- Malo, L., Doyon, R., Lafrenière, D., et al. 2013, *ApJ*, 762, 88
- Malo, L., Artigau, É., Doyon, R., et al. 2014, *ApJ*, 788, 81
- Mamajek, E. E., Lawson, W. A., & Feigelson, E. D. 1999, *ApJL*, 516, L77
- Mamajek, E. E. 2005, *ApJ*, 634, 1385.
- Marois, C., Macintosh, B., Barman, T., et al. 2008, *Science*, 322, 1348
- Marois, C., Zuckerman, B., Konopacky, Q. M., Macintosh, B., & Barman, T. 2010, *Nature*, 468, 1080
- Massey, P., & Olsen, K. A. G. 2003, *AJ*, 126, 2867
- Meng, H. Y. A., Rieke, G. H., Su, K. Y. L., & Gáspár, A. 2017, *ApJ*, 836, 34
- Mentuch, E., Brandeker, A., van Kerkwijk, M. H., Jayawardhana, R., & Hauschildt, P. H. 2008, *ApJ*, 689, 1127
- Messina, S., Lanzafame, A. C., Malo, L., et al. 2017, *A&A*, 607, A3
- Mochnicki, S. W., Gladders, M. D., Thomson, J. R., et al. 2002, *AJ*, 124, 2868
- Montes, D., López-Santiago, J., Gálvez, M. C., et al. 2001, *MNRAS*, 328,
- Moór, A., Szabó, G. M., Kiss, L. L., et al. 2013, *MNRAS*, 435, 1376
- Murphy, S. J., Lawson, W. A., & Bessell, M. S. 2013, *MNRAS*, 435, 1325
- Murphy, S. J., Lawson, W. A., & Bento, J. 2015, *MNRAS*, 453, 2220
- Murphy, S. J., & Lawson, W. A. 2015, *MNRAS*, 447, 1267
- Murphy, S. J., Mamajek, E. E., & Bell, C. P. M. 2018, *MNRAS*, 476, 3290
- Naud, M.-E., Artigau, É., Malo, L., et al. 2014, *ApJ*, 787, 5
- Nefs, S. V., Birkby, J. L., Snellen, I. A. G., et al. 2012, *MNRAS*, 425, 950
- Newton, E. R., Charbonneau, D., Irwin, J., et al. 2014, *AJ*, 147, 20
- Nordström, B., Mayor, M., Andersen, J., et al. 2004, *A&A*, 418, 989
- Ochsenbein, F. 1980, *Bulletin d'Information du Centre de Donnees Stellaires*, 19, 74
- Oh, S., Price-Whelan, A. M., Hogg, D. W., Morton, T. D., & Spergel, D. N. 2017, *AJ*, 153, 257
- Pecaut, M. J., & Mamajek, E. E. 2013, *The Astrophysical Journal Supplement Series*, 208, 9
- Pecaut, M. J., & Mamajek, E. E. 2016, *MNRAS*, 461, 794
- Rebull, L. M., Stapelfeldt, K. R., Werner, M. W., et al. 2008, *ApJ*, 681, 1484
- Reid, I. N., Hawley, S. L., & Gizis, J. E. 1995, *AJ*, 110, 1838
- Reid, I. N., Cruz, K. L., Allen, P., et al. 2003, *AJ*, 126, 3007
- Reid, I. N., Cruz, K. L., Allen, P., et al. 2004, *AJ*, 128, 463
- Reiners, A., & Basri, G. 2009, *ApJ*, 705, 1416
- Reiners, A., Zechmeister, M., Caballero, J. A., et al. 2018, *A&A*, 612, A49
- Reylé, C., Scholz, R.-D., Schultheis, M., et al. 2006, *MNRAS*, 373, 705
- Riaz, B., Gizis, J. E., & Harvin, J. 2006, *AJ*, 132, 866
- Riedel, A. R., Finch, C. T., Henry, T. J., et al. 2014, *AJ*, 147, 85

- Riedel, A. R., Alam, M. K., Rice, E. L., Cruz, K. L., & Henry, T. J. 2017, *ApJ*, 840, 87
- Riviere-Marichalar, P., Barrado, D., Montesinos, B., et al. 2014, *A&A*, 565, A68
- Rizzuto, A. C., Ireland, M. J., & Robertson, J. G. 2011, *MNRAS*, 416, 3108
- Rodriguez, D. R., Bessell, M. S., Zuckerman, B., et al. 2011, *ApJ*, 727, 62
- Rodriguez, D. R., Zuckerman, B., Kastner, J. H., et al. 2013, *ApJ*, 774, 101
- Rodriguez, D. R., van der Plas, G., Kastner, J. H., et al. 2015, *A&A*, 582, L5
- Sacco, G. G., Flaccomio, E., Pascucci, I., et al. 2012, *ApJ*, 747, 142
- Schlieder, J. E., Lépine, S., Rice, E., et al. 2012, *AJ*, 143, 114.
- Schneider, A., Song, I., Melis, C., et al. 2012, *ApJ*, 757, 163
- Schneider, A. C., Windsor, J., Cushing, M. C., Kirkpatrick, J. D., & Shkolnik, E. L. 2017, *AJ*, 153, 196
- Schneider, A. C., & Shkolnik, E. L. 2018, *AJ*, 155, 122
- Scholz, R.-D., Lo Curto, G., Méndez, R. A., et al. 2005, *A&A*, 439, 1127
- Seifahrt, A., Reiners, A., Almaghrbi, K. A. M., et al. 2010, *A&A*, 512, A37
- Shan, Y., Yee, J. C., Bowler, B. P., et al. 2017, *ApJ*, 846, 93
- Shkolnik, E., Liu, M. C., & Reid, I. N. 2009, *ApJ*, 699, 649
- Shkolnik, E. L., Liu, M. C., Reid, I. N., Dupuy, T., & Weinberger, A. J. 2011, *ApJ*, 727, 6
- Shkolnik, E. L., & Barman, T. S. 2014, *AJ*, 148, 64
- Shkolnik, E. L., Allers, K. N., Kraus, A. L., Liu, M. C., & Flagg, L. 2017, *AJ*, 154, 69
- Silverberg, S. M., Kuchner, M. J., Wisniewski, J. P., et al. 2016, *ApJL*, 830, L28
- Song, I., Bessell, M. S., & Zuckerman, B. 2002, *A&A*, 385, 862
- Song, I., Zuckerman, B., & Bessell, M. S. 2004, *ApJ*, 600, 1016
- Song, I., Zuckerman, B., & Bessell, M. S. 2012, *AJ*, 144, 8
- Soubiran, C., Jasiewicz, G., Chemin, L., et al. 2018, *A&A*, 616, A7
- Sperauskas, J., Bartašiūtė, S., Boyle, R. P., et al. 2016, *A&A*, 596, A116
- Stocke, J. T., Morris, S. L., Gioia, I. M., et al. 1991, *The Astrophysical Journal Supplement Series*, 76, 813
- Strassmeier, K., Washuettl, A., Granzer, T., et al. 2000, *Astronomy and Astrophysics Supplement Series*, 142, 275
- Su, K. Y. L., Rieke, G. H., Stansberry, J. A., et al. 2006, *ApJ*, 653, 675
- Terrien, R. C., Mahadevan, S., Bender, C. F., et al. 2015a, *ApJ*, 802, L10
- Terrien, R. C., Mahadevan, S., Deshpande, R., & Bender, C. F. 2015b, *ApJS*, 220, 16
- Thackrah, A., Jones, H., & Hawkins, M. 1997, *MNRAS*, 284, 507
- Tian, H.-J., Gupta, P., Sesar, B., et al. 2017, *ApJS*, 232, 4
- Torres, C. A. O., da Silva, L., Quast, G. R., et al. 2000, *AJ*, 120, 1410
- Torres, C. A. O., Quast, G. R., de La Reza, R., da Silva, L., & Melo, C. H. F. 2001, *Young Stars Near Earth: Progress and Prospects*, 244, 43
- Torres, C. A. O., Quast, G. R., da Silva, L., et al. 2006, *A&A*, 460, 695
- Torres, C. A. O., Quast, G. R., Melo, C. H. F., & Sterzik, M. F. 2008, *Handbook of Star Forming Regions, Volume II*, 5, 757
- Truemper, J. 1982, *Advances in Space Research*, 2, 241
- Ugrena, A. R., & Harlow, J. J. B. 1996, *PASP*, 108, 64
- van der Marel, N., Verhaar, B. W., van Terwisga, S., et al. 2016, *A&A*, 592, A126
- Viana Almeida, P., Santos, N. C., Melo, C., et al. 2009, *A&A*, 501, 965
- Vogt, S. S., Allen, S. L., Bigelow, B. C., et al. 1994, *Proc. SPIE*, 2198, 362
- Weinberg, M. D., Shapiro, S. L., & Wasserman, I. 1987, *ApJ*, 312, 367
- West, A. A., Hawley, S. L., Bochanski, J. J., et al. 2008, *AJ*, 135, 785
- West, A. A., Morgan, D. P., Bochanski, J. J., et al. 2011, *AJ*, 141, 97
- West, A. A., Weisenburger, K. L., Irwin, J., et al. 2015, *ApJ*, 812, 3
- White, R. J., & Basri, G. 2003, *ApJ*, 582, 1109
- Wilson, O. C. 1967, *AJ*, 72, 905
- Winters, J. G., Sevrinsky, R. A., Jao, W.-C., et al. 2017, *AJ*, 153, 14
- Woolley, R., Epps, E. A., Penston, M. J., et al. 1970, *Royal Observatory Annals*, 5, ill
- Wright, C. O., Egan, M. P., Kraemer, K. E., et al. 2003, *AJ*, 125, 359
- Zacharias, N., Finch, C. T., Girard, T. M., et al. 2013, *AJ*, 145, 44
- Zacharias, N., Finch, C., & Frouard, J. 2017, *AJ*, 153, 166
- Žerjal, M., Ireland, M. J., Nordlander, T., et al. 2019, *MNRAS*, 484, 4591
- Zhong, J., Lépine, S., Li, J., et al. 2015, *Research in Astronomy and Astrophysics*, 15, 1154
- Zuckerman, B., Webb, R. A., Schwartz, M., et al. 2001a, *ApJ*, 549, L233.
- Zuckerman, B., Song, I., & Webb, R. A. 2001b, *ApJ*, 559, 388

Zuckerman, B., Bessell, M. S., Song, I., & Kim, S. 2006,  
ApJL, 649, L115

Zuckerman, B., Rhee, J. H., Song, I., & Bessell, M. S. 2011,  
ApJ, 732, 61  
Zuckerman, B. 2019, ApJ, 870, 27